

4613-105-T

AD 669833

Report of BAMIRAC

**MEASUREMENT OF
THE TIME-VARYING COMPONENT
OF RADIATION FROM INFRARED SOURCES**

E. C. HALL
M. L. FECTEAU
C. L. ROE



INFRARED PHYSICS LABORATORY

William P. Slichter Laboratories
THE INSTITUTE OF SCIENCE AND TECHNOLOGY

May 1968

Prepared for Advanced Research Projects Agency,
Department of Defense, Washington, D. C., Contract SD-91

This document has been approved for public release and sale;
its distribution is unlimited.

Reproduced by the
CLEARINGHOUSE
for Federal Scientific & Technical
Information Springfield Va. 22151

NOTICES

Sponsorship. The work reported herein is a part of the research under **BAMIRAC** (Ballistic Missile Research Analysis Center) conducted at the Willow Run Laboratories of the Institute of Science and Technology for the Advanced Research Projects Agency, Department of Defense, under Contract SD-91 (ARPA Order 236) as a part of Project DEFENDER (research on defense against ballistic missiles). Contracts and grants to The University of Michigan for the support of sponsored research are administered through the Office of the Vice-President for Research.

BAMIRAC. The Ballistic Missile Radiation Analysis Center is specifically concerned with electromagnetic radiation emanating from or caused by ICBM's or IRBM's in the powered and ballistic phases. In accordance with DOD Instruction 5100.45, BAMIRAC collects, processes, and disseminates information obtained from reports of field measurements and from laboratory and theoretical studies. In addition, it conducts its own theoretical and experimental investigations. From information so obtained, models are developed to relate observed radiations to physical causes. These models are published in the Center's annual and semiannual reports. Other publications include technical papers, state-of-the-art reports, and missile measurement résumés. BAMIRAC provides for visits of qualified persons and prepares bibliographies on request. Also, the facility aids ARPA by planning and conducting various technical conferences and by publishing the Proceedings of the Anti-Missile Research Advisory Council.

BAMIRAC is under the technical direction of the Infrared Physics Laboratory of the Willow Run Laboratories, a unit of The University of Michigan's Institute of Science and Technology. It draws also upon the capabilities of the Infrared and Optical Sensor Laboratory and the Computation Department of Willow Run Laboratories, and upon those of the Gas Dynamics Laboratory of the Department of Aerospace Engineering and of other departments of The University of Michigan, particularly within the College of Engineering.

Distribution. Initial distribution of this report has been approved by the Advanced Research Projects Agency and is indicated at the end of this document.

DDC Availability. Qualified requesters may obtain copies of this document from

Defense Documentation Center
Cameron Station
Arlington, Virginia 22314

Final Disposition. After this document has served its purpose, it may be destroyed. Please do not return it to Willow Run Laboratories.

REVISION for	
WST	WHITE SECTION
ISG	DIFF SECTION
UNANNOUNCED JUSTIFICATION	
BY	
DISTRIBUTION/AVAILABILITY CODE	
1ST.	AVAIL. and/or SPEC.

4613-105-T

Report of BAMIRAC

**MEASUREMENT OF
THE TIME-VARYING COMPONENT
OF RADIATION FROM INFRARED SOURCES**

E. C. HALL
M. L. FECTFAU
C. L. ROE

May 1968

Infrared Physics Laboratory
Willow Run Laboratories
THE INSTITUTE OF SCIENCE AND TECHNOLOGY
THE UNIVERSITY OF MICHIGAN
Ann Arbor, Michigan

This document has been approved for public release and sale;
its distribution is unlimited.

ABSTRACT

Techniques for the calibration of a temporal radiometer have been studied. The calibration described for either periodic or random fluctuations utilizes sinusoidally modulated radiation from a blackbody. A complete description is given of the data acquisition and analysis facilities which were assembled for this study and used to calibrate a test radiometer. The practical aspects of spectral analysis (including the interplay among filter bandwidth, scan rate, data sample length, and averaging time) are discussed, and a technique for measuring the noise equivalent bandwidth of the frequency-selective filter in the spectrum analyzer is described.

BLANK PAGE

WILLOW RUN LABORATORIES

CONTENTS

Abstract	iii
List of Figures.	vi
List of Tables	vi
1. Introduction.	1
2. Basic Approach.	1
3. Calibration Procedure	6
3.1. Instrument Description	6
3.2. Responsivity Determination	7
3.3. Temporal Radiance Source	10
3.4. Other Sources of Modulated Radiation	10
3.5. Sample Calibration	12
3.6. Square Wave Modulated Source Calibration Check	16
4. Summary and Conclusion	21
Appendix I: Instrumentation.	23
Appendix II: Practical Aspects of Power Spectral Density Analysis	25
Appendix III: Calibration of Spectrum Analyzer for Direct Power Spectral Density Measurements	34

WILLOW RUN LABORATORIES

FIGURES

1. Typical Temporal Radiometer	2
2. Sinusoidally Chopped Blackbody Source	11
3. Exploded View of Calibration Source	11
4. Relative GaAs Spectrum	13
5. Relative Glow Modulator Spectrum Type R1130B	14
6. Relative Spectral Responsivity	15
7. Relative Spatial Responsivity	15
8. Temporal Irradiance Responsivity	16
9. Temporal Irradiance Responsivity as a Function of Frequency.	17
10. Precision Square Wave Chopper	18
11. Sample Data-Frequency Analysis of 45-Hz Square Wave	20
12. Radiometers Without Rear Covers	24
13. Continuous-Loop Playback System	24
14. Typical Power Spectrum	27
15. Spectrum Analyzer Block Diagram	27
16. Chi-Square Distribution Chart.	28
17. Typical Filter Curve	36
18. Calibration Block Diagram	36
19. Response of 2-Hz Filter	38
20. Response of 20-Hz Filter	38
21. Response of 200-Hz Filter.	38
22. Power Spectral Density Measurements for Three Filters	40

TABLES

I. Harmonic Distortion Measurements.	12
II. Analysis of 180-Hz Square Wave	19
III. Parameters for Data Reduction System	32
IV. TP-626 Oscillator Sweep Intervals per 100 Seconds	36
V. Bandwidth Divisor Settings	39

MEASUREMENT OF THE TIME-VARYING COMPONENT OF RADIATION FROM INFRARED SOURCES

1 INTRODUCTION

Temporal radiometry, the measurement of the fluctuating component of infrared radiation associated with targets of various types, has become increasingly important in recent years. For such measurements, the instruments and experimental techniques can differ greatly from those of conventional radiometry where the concern is only the measurement of a time-averaged quantity. Of course, the time-averaged quantity is averaged only over a finite length of time. Thus any radiation fluctuation slower than the integration time will not be averaged out and will appear as slow variations of the (time-averaged) output. Conventional radiometry and temporal radiometry are therefore not mutually exclusive, so that the division becomes somewhat arbitrary. We will assume in the following discussion that temporal radiometry is the study of fluctuations above, say, 5 Hz.

The fluctuations of concern in this study are, ultimately, modulations of carrier frequencies, i.e., radiation frequencies. However, the magnitudes of these two sets of frequencies and the mechanism that gives rise to the modulation differ so greatly that the two sets of frequencies are effectively uncoupled. Accordingly, the following definitions apply in this report:

Modulation means a time-varying component superimposed on a positive steady-state value of the radiant quantity.

Frequency means the processed temporal content of the signal.

Wavelength means the spectral content of the signal.

The field of temporal radiometry has grown rapidly, and, the number of investigations of target and background characteristics (including earth and sky backgrounds) is considerable [1-13]. However, relatively little effort has been devoted to establishing proper calibration and data reduction procedures. In fact, analysis of some of the more recent temporal radiometric data indicated a lack of quantitative presentation and differences in techniques employed by various investigators, which made it impossible to fully ascertain the significance of many of the experimental data. For this reason, and in view of the potential importance of such measurements, a study was undertaken with the objective of developing methods for the absolute calibration of such instruments.

2
BASIC APPROACH

The analysis of time-varying data in terms of a distribution in frequency affords a reduction of a large if not unmanageable amount of raw data into a convenient and sometimes more significant form. The mathematical techniques for such analysis have long been available and are thoroughly discussed in a number of current publications [14-20]. However, the application of spectral analysis techniques to practical problems, in particular temporal radiometry, is not always straightforward.

Consider the behavior of each of the following components that constitute a typical radiometer (fig. 1):

- (a) The optical system and filter, which collect and focus spectrally selected unchopped radiation upon the detector.

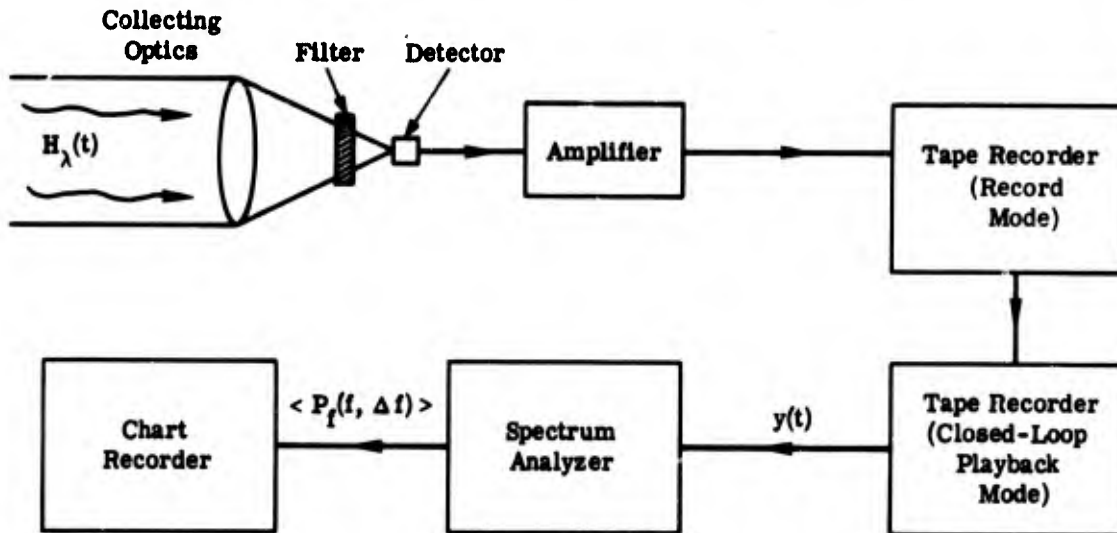


FIGURE 1. TYPICAL TEMPORAL RADIOMETER

- (b) The detector, which transduces the input signal (time-varying infrared radiation) into an output signal voltage.
- (c) Electronics, which amplify this signal to a suitable level for recording on magnetic tape.
- (d) A spectrum analyzer, which processes the tape-recorded signal and yields the final output, a chart recording of the distribution in frequency of some quantity related to the input.

In principle, we could measure the transfer function (output divided by input) of these components separately and thereby deduce the response characteristics of the entire system. Alternatively, the entire system can be calibrated in terms of an input radiant power and an output frequency distribution only. The latter approach is more in keeping with standard radiometric practice and was therefore adopted for the present investigation. An effort was also made to retain as much of the usual radiometric notation and terminology as possible.

The purpose in calibrating a temporal radiometer is to obtain the distribution in frequency of some function $\psi_f \equiv \partial\psi/\partial f$, such that

$$\psi(\Delta\lambda, \Delta f) = \int_{f_1}^{f_2} \psi_f df \quad (1)$$

where $\psi(\Delta\lambda, \Delta f)$ is a quantity related to the time-varying irradiance at the entrance of the radiometer in the spectral (wavelength) interval $\Delta\lambda$ and modulation frequency interval $\Delta f = f_2 - f_1$. In other words, the calibration must provide the means for labeling the ordinate of the spectrum analyzer output in terms of radiant power input, so the area under any part of the distribution curve, ψ_f vs. f , represents an absolute radiometric quantity expressible in terms of units such as watts per square centimeter.

The above procedure is analogous to the absolute calibration of a spectrometer to obtain a distribution in wavelength of input spectral irradiance, $H_\lambda \equiv \partial H/\partial\lambda$ vs. λ , which yields upon integration the irradiance in the specified interval $\Delta\lambda$. The narrowband filter-response characteristic in the analyzer corresponds in a sense to the slit function in a spectrometer. It is well known that, because of finite resolution, only the irradiance in a narrow range of wavelengths can be measured:

$$H(\Delta\lambda) \equiv \int_{\Delta\lambda} H_\lambda d\lambda \quad [\text{w-cm}^{-2}]$$

To overcome this difficulty, the average spectral irradiance (an "estimate" of the true spectral irradiance) is defined as

$$\bar{H}_\lambda(\lambda, \Delta\lambda) \equiv \frac{1}{\Delta\lambda} \int_{\Delta\lambda} H_\lambda d\lambda \quad [\text{w-cm}^{-2}\text{-}\mu^{-1}]$$

Now, if a limiting process is performed:

$$\lim_{\Delta\lambda \rightarrow 0} \bar{H}_\lambda(\lambda, \Delta\lambda) = \lim_{\Delta\lambda \rightarrow 0} \frac{1}{\Delta\lambda} \int_{\Delta\lambda} H_\lambda d\lambda \equiv H_\lambda(\lambda)$$

it is seen that the "estimate" of spectral irradiance by definition becomes the desired true spectral irradiance. It is worth noting that we never speak of the irradiance at a particular wavelength, because the amount of irradiance at a single wavelength is vanishingly small.

As already mentioned, the techniques of analysis in the frequency domain are well developed, but only a few authors, most notably Jones [14, 21], have applied the techniques of electrical noise analysis to radiometry. The function considered basic to such analysis is the power spectral density function, $P_f(f)$, defined as [15]

$$P_f(f) \equiv \lim_{\Delta f \rightarrow 0} \lim_{T \rightarrow \infty} \frac{1}{T \Delta f} \int_0^T y_{\Delta f}^2(t) dt \quad [v^2 - Hz^{-1}] \quad (2)$$

$T \Delta f \rightarrow \infty$

where $y_{\Delta f}^2(t)$ is the square of the instantaneous amplitudes in the narrow frequency bandwidth Δf , and T is an integration time. On integration, equation 2 yields the electrical power in the bandwidth Δf :*

$$P(\Delta f) \equiv \int_{\Delta f} P_f(f) df \quad [v^2]$$

The "estimate" of $P_f(f)$, analogous to the "estimate" of H_λ above, is

$$\langle P_f(f, \Delta f, T) \rangle \equiv \frac{1}{T \Delta f} \int_0^T y_{\Delta f}^2(t) dt \quad [v^2 - Hz^{-1}] \quad (3)$$

where angular brackets indicate time averaging. Depending on the choice of integration time T and bandwidth Δf , the accuracy of the "estimate" can be determined. (See appendix II for a more detailed discussion of the proper choice of T and Δf .)

The name "power spectral density" can lead to some confusion since, in radiometry, a voltage is proportional to radiant power. Here we are working with a voltage squared per unit of frequency, which must, of course, be proportional to radiant power squared per unit frequency in units such as watts squared per Hertz.

No radiation source randomly modulated at audio frequencies is available for the absolute calibration of radiometers to be used to study random fluctuations; therefore, specialization of the above theory to account for periodic signals is desirable. Furthermore, a sinusoidally modulated radiation source can easily be constructed (see sec. 3.3). Let us, therefore, consider the consequences to equation 3 of using a periodically varying source.

*Power across a 1-ohm resistor is numerically equal to the squared voltage, hence the identification of electrical power with volts squared.

By rearranging, equation 3 can be written

$$\langle P_f(f, \Delta f, T) \rangle \Delta f = \frac{1}{T} \int_0^T y_{\Delta f}^2(t) dt \quad [v^2] \quad (4)$$

But the integral on the right of equation 4 is proportional to the average electrical power in a narrow bandwidth Δf , i.e., $P(\Delta f)$. For a periodic signal which has only one component contained within the electrical filter bandwidth Δf , it is known that the electrical power is independent of Δf , so that we may write

$$P(\Delta f) = \langle P_f(f, \Delta f, T) \rangle \Delta f = \frac{1}{T} \int_0^T y_{\Delta f}^2(t) dt = \text{a constant} \quad [v^2] \quad (5)$$

independent of Δf . (Note that, in this special case, we may speak of power at a particular frequency, f_0 , independent of bandwidth).

It follows that, for perfectly periodic signals, $P_f(f) \equiv \partial P / \partial f$ must be a constant times a delta function:

$$P \int \delta(f - f_0) df = \lim_{T \rightarrow \infty} \frac{1}{T} \int_0^T y_{\Delta f}^2(t) dt \quad [v^2]$$

where $\delta(f - f_0)$ is a Dirac delta function, defined only at f_0 such that

$$\int_{-\infty}^{\infty} \delta(x - x_0) dx = 1$$

Thus, equation 2 is meaningless for periodic signals, since $P_f(f)$ is essentially a delta function.* Consequently, to use a periodic source to calibrate temporal radiometers for both periodic and random fluctuating signals, we will have to write

$$\langle P_f(f, \Delta f, T) \rangle \Delta f = \frac{1}{T} \int_0^T y_{\Delta f}^2(t) dt \propto \langle H^2(f, \Delta f, T) \rangle \quad (6)$$

where the constant of proportionality is the temporal irradiance responsivity R_H :

$$R_H(f, \Delta f, T, \dots) \equiv \frac{\langle P_f(f, \Delta f, T, \dots) \rangle \Delta f}{\langle H^2(f, \Delta f, T, \dots) \rangle} \quad [v^2 / (w\text{-cm}^{-2})^2] \quad (7)$$

in which (...) indicates dependence on other variables.

*Of course, no real function is perfectly periodic and therefore never a true delta function. However, if the signal is sampled for a period of time 10 times the reciprocal of the limiting filter's bandwidth, the error in assuming that the signal is perfectly periodic is usually negligible.

The extension to random signals is now straightforward. Since electrical power has meaning for both random and periodic signals, it follows that

$$\langle H^2(f, \Delta f, T, \dots) \rangle = \frac{\langle P_f(f, \Delta f, T, \dots) \rangle \Delta f}{R_H(f, \Delta f, T, \dots)} [(w\text{-cm}^{-2})^2] \quad (8)$$

regardless of the signal type. If the signal is random (electrical power is directly proportional to bandwidth), we can speak of either the mean square irradiance density in the bandwidth Δf :

$$\frac{\partial H^2}{\partial f} = H_f^2 = \frac{\langle H^2(f, \Delta f, T, \dots) \rangle}{\Delta f} = \frac{\langle P_f(f, \Delta f, T, \dots) \rangle}{R_H(f, \Delta f, T, \dots)} [(w\text{-cm}^{-2})^2 \text{-Hz}^{-1}] \quad (9)$$

or the rms irradiance density:*

$$\frac{\langle H^2(f, \Delta f, T, \dots) \rangle^{1/2}}{\sqrt{\Delta f}} = \left[\frac{\langle P_f(f, \Delta f, T, \dots) \rangle}{R_H(f, \Delta f, T, \dots)} \right]^{1/2} [w\text{-cm}^{-2} \text{-Hz}^{-1/2}] \quad (10)$$

One more point should be made. The electric filter bandwidth Δf is not the nominal filter bandwidth but rather the "noise equivalent" bandwidth. This accounts for the nonideal filter shape and is somewhat analogous to the slit-function correction in spectroscopy. The measurement of the noise equivalent bandwidth is the subject of appendix III.

3

CALIBRATION PROCEDURE

3.1. INSTRUMENT DESCRIPTION

In this report, a temporal radiometer (fig. 1) will be taken to consist of an optical system with a detector, an amplifier, a magnetic tape recorder, a spectrum analyzer, and a chart recorder. The infrared radiation at the entrance aperture of the instrument, $H(t, \lambda)$, will be considered to be a function of time and wavelength only. For an effective spectral bandwidth $\Delta\lambda$, the signal voltage out of the detector $E(t, \Delta\lambda)$, in general a linear function of the irradiance $H(t, \Delta\lambda)$, is amplified to a suitable level and recorded on magnetic tape. For analysis, a segment of the magnetic tape representing a time interval Δt is formed into a closed loop; an appropriate frequency analysis is performed by the spectrum analyzer and the results are displayed on the chart recorder.

That is, the square root of the mean square irradiance density. This expression is similar to the inverse of D^ , discussed by Jones [21].

3.2. RESPONSIVITY DETERMINATION

Consider a blackbody source capable of emitting radiation that varies sinusoidally.* The spectral irradiance at the entrance aperture of a radiometer illuminated by this source would be given by

$$H_{\lambda}(t) = \frac{N_{\lambda}}{2} [1 + \sin 2\pi f_c t] \frac{A}{d^2} \tau(\lambda) \quad [\text{w-cm}^{-2}\text{-}\mu^{-1}] \quad (11)$$

where N_{λ} is the spectral radiance of the blackbody, $N_{\lambda}/2$ represents the d-c or time-averaged level, f_c is the chopping frequency, A is the maximum exposed area of the blackbody, d is the distance between the source and the receiver, and $\tau(\lambda)$ is the transmittance of the intervening atmosphere. Since the radiometer does not respond to all the radiation at the entrance aperture, but only to that portion of the radiation within the spectral bandpass of the instrument, it is useful to define an effective irradiance as

$$H(\Delta\lambda, t) = \int_{\Delta\lambda} H_{\lambda}(t) s(\lambda) d\lambda \quad [\text{w-cm}^{-2}] \quad (12)$$

where $s(\lambda)$ is the relative spectral response of the optical elements and detector.

Since the power spectrum mode of analyzer operation is to be used for presenting the frequency distribution of random time-varying inputs, the quantity of interest in the calibration of a temporal radiometer is the mean square irradiance value,† defined as

$$\langle H^2(\Delta\lambda) \rangle = \frac{1}{T} \int_0^T H^2(\Delta\lambda, t) dt \quad [(\text{w-cm}^{-2})^2] \quad (13)$$

where T in this case is the period. By combining equations 11 and 12 and dropping the d-c term from (11) because a temporal radiometer is not usually designed to respond to it,

$$\langle H^2(\Delta\lambda) \rangle = \frac{A^2}{8d^4} \left[\int_{\Delta\lambda} N_{\lambda} \tau(\lambda) s(\lambda) d\lambda \right]^2 \quad (14)$$

All of the parameters in equation 14 are known or can be measured for the particular experimental conditions. Thus we can determine the value of the mean square irradiance, which is independent of the chopping frequency f_c . The detector and amplifier must be linear, so that the signal, $E(t)$, recorded on magnetic tape is proportional to the effective irradiance $H(\Delta\lambda, t)$.

*See section 3.3 for a description of such a calibration source.

†These units are in keeping with the method developed by R. C. Jones [14] for describing the statistical variation of background signals.

A segment of the data recording is then selected for frequency analysis via the closed-loop tape playback and the spectrum analyzer. To make the signal correspond to the mean square irradiance (eq. 14), it is processed to yield $\langle P_f(f_c, \Delta f) \rangle \Delta f$ volts², the electrical power for the input voltage $E(t)$ in the following manner:

$$\langle P_f(f_c, \Delta f, T) \rangle \Delta f = \frac{1}{T} \int_0^T E^2(t) dt \quad [v^2] \quad (15)$$

where Δf is the bandwidth of the filter centered at f_c (the chopping frequency) and T is an integration time. Note that, for this particular calibration, $E(t) = E_0 \cos 2\pi f_c t$, and $E^2(t) = E_0^2 \cos^2 2\pi f_c t$, so that

$$\langle P_f(f_c, \Delta f) \rangle \Delta f = E_0^2/2$$

where E_0 is the peak amplitude at frequency f_c . But for the sake of generality and also since the analyzer indicates either power or power density directly, we will retain the left-hand expression for the remainder of this discussion.

The temporal responsivity factor is defined as

$$R_H(f_c, \Delta f, \Delta\lambda) = \frac{\langle P_f(f_c, \Delta f) \rangle \Delta f}{\langle H^2(\Delta\lambda) \rangle} = \frac{\langle P_f(f_c, \Delta f) \rangle \Delta f}{(A^2/8D^4) \left[\int N_\lambda \tau(\lambda) s(\lambda) d\lambda \right]^2} \quad [v^2/(w\text{-cm}^{-2})^2] \quad (16)$$

Equation 16 yields the temporal responsivity at one specific frequency, f_c , and for the particular electrical gain setting, electrical bandwidth Δf , and optical bandwidth $\Delta\lambda$. It is, of course, necessary that all the instrument settings, with the possible exception of the electrical gain setting, be the same during both calibration and target measurements.

It would be desirable to repeat the calibration procedure over the complete range of frequencies normally covered in the power spectral density plots. However, the limitation on the range of easily obtainable chopping frequencies may prevent such a measurement. In such cases other sources, such as semiconductor diodes, are available; they do not suffer a reduction in the emitted radiation over most of the frequency ranges of interest (sec. 3.2). These sources can be used to measure the relative temporal responsivity, and, through the following equation, the absolute temporal responsivity can be computed for all frequencies of interest:

$$R_H(f, \Delta f, \Delta \lambda) = R_{H_c}(f_c, \Delta f, \Delta \lambda) \frac{r(f)}{r(f_c)} [v^2 / (w\text{-cm}^{-2})^2] \quad (17)$$

where $r(f)$ is the relative temporal responsivity measured with the nonquantitative source.

For computing the mean square irradiance per unit bandwidth as a function of frequency for some target, equation 16 is rearranged as

$$\langle H_f^2(\Delta f, \Delta \lambda) \rangle = \frac{k^2 \langle P(f, \Delta f) \rangle}{R_{ii}(f, \Delta f, \Delta \lambda)} [(w\text{-cm}^{-2})^2 \text{-Hz}^{-1}] \quad (18)$$

where $\langle P(f, \Delta f) \rangle$ is the power density (i.e., volts²-Hz⁻¹) and k is a factor which accounts for any gain introduced into the electronics between calibration and measurement when the power spectrum is computed. From our previous discussion we know that any periodic fluctuations of the target will show up as a strong spike in the plot of $\langle H_f^2(\Delta f, \Delta \lambda) \rangle$ vs. frequency.

A complete description of the target must also include measurement of the mean irradiance level, $\langle H(\Delta \lambda) \rangle$, so that a modulation ratio can be determined. Consider a band of frequencies $f_2 - f_1 \gg \Delta f$. A modulation ratio can be defined as:

$$M(f_2 - f_1, \Delta \lambda) = \frac{\left[\int_{f_1}^{f_2} \langle H_f^2(\Delta f, \Delta \lambda) \rangle df \right]^{1/2}}{\langle H(\Delta \lambda) \rangle} \quad (19)$$

The mean irradiance level, $\langle H(\Delta \lambda) \rangle$, should be measured with a radiometer having its band-pass, $\Delta \lambda$, and field of view as nearly identical as possible but including a chopper and synchronous rectification.

Because the intensity of time-varying radiation and the time-averaged radiation can differ by an order of magnitude or more, inadvertant operation of the detector in a nonlinear mode can result in considerable error; measurements on a PbS detector have shown this can occur when the d-c levels are sufficiently large to cause saturation. For this reason it is advisable to measure the output of the temporal radiometer over the complete intensity range of the time-varying and time-averaged signals expected to be encountered in the target measurements.

The relative spatial responsivity (field of view) is a parameter that must be carefully determined as part of the instrument calibration because of the manner in which the temporal variation is introduced during calibration, i.e., by continuously changing the covered portion of a shaped aperture in front of a blackbody. These measurements must show negligible variation in response throughout the regions in the field of view occupied by the calibration source and the targets.

The techniques for measuring the relative spectral responsivity and the relative spatial responsivity are described in various publications [22, 23]. The only difference in temporal radiometry is that the source must be modulated. The modulation frequency can be any convenient value, provided it is within the passband of the electronics.

3.3. TEMPORAL RADIANCE SOURCE

The sinusoidally modulated blackbody, used as an absolute calibration source and hereafter referred to as the "temporal radiance" standard, is shown in figures 2 and 3. The blackbody itself is a commercial unit;* the aperture and chopper design were reported by W. Wallin [24]. Measurements of the bandwidth of the "line" generated by the temporal radiance standard indicated it to be less than 1% of the center frequency. The intensity of this "temporal emission" line can be varied by simply changing the temperature of the blackbody cavity. The frequency of the emission line can be varied by a change of pulleys; the unit pictured in figure 2 has a range from 20 to 260 Hz.

The harmonic distortion was measured at a number of frequencies from 20 to 260 Hz. The total harmonic distortion is defined as:

$$D = \frac{[|V_2|^2 + |V_3|^2 + \dots]^{1/2}}{V_1}$$

where D is the harmonic distortion and V_1 , V_2 , and V_3 are the amplitude of the fundamental, second, and third harmonics, etc. The measurements, summarized in table I, indicate negligible variation with the fundamental frequency, as might be expected. Considerable care had to be taken in aligning the unit, both internally and with respect to the radiometer, because the beam of radiation was easily vignetted. The pulleys and motor (fig. 2) were frequently exposed during a calibration. Baffling the radiation from the motor and other moving parts was unnecessary for operation in the PbS region but would be required for operation at the longer wavelengths.

3.4. OTHER SOURCES OF MODULATED RADIATION

The major shortcoming of the temporal radiance standard pictured in figure 2 is the available frequency range, the upper limit of which in this experiment was 260 Hz. The frequency limit could have been extended to somewhat higher values. However, other sources can be used to obtain the relative temporal responsivity and thereby a complete calibration of the radiometer.

*Barnes Engineering Co., Model 11-201.

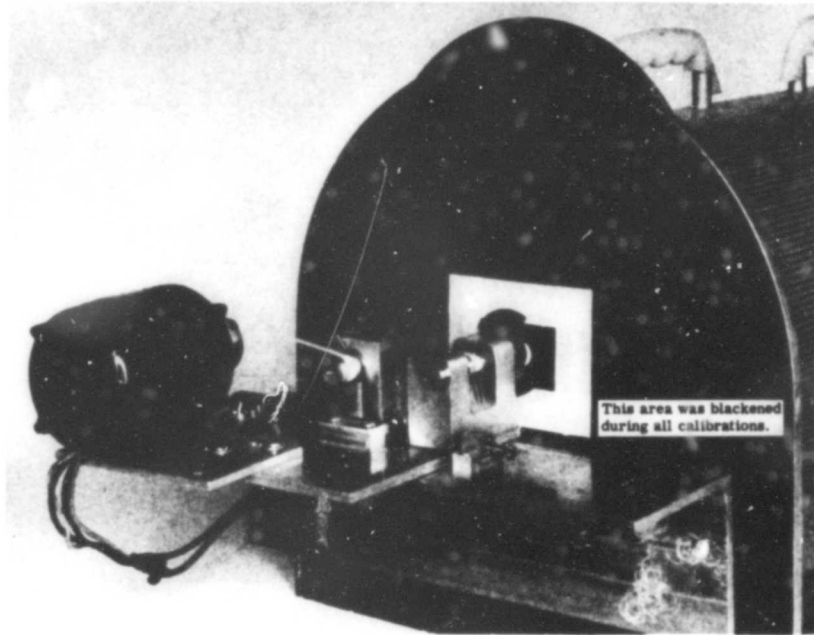


FIGURE 2. SINUSOIDALLY CHOPPED BLACKBODY SOURCE

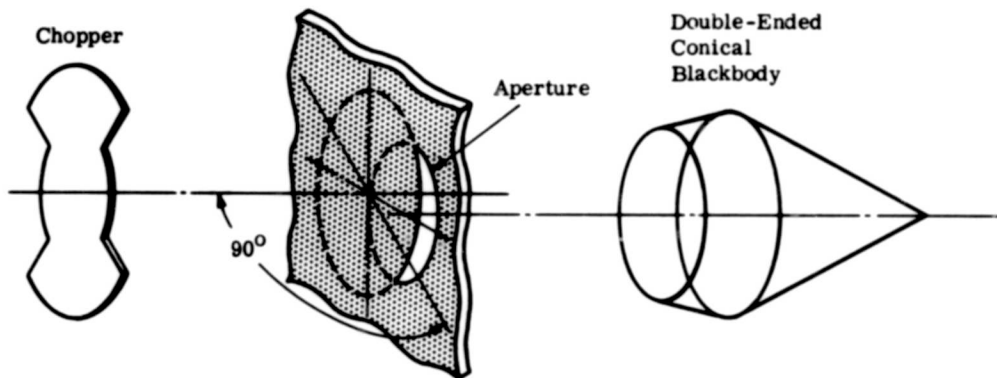


FIGURE 3. EXPLODED VIEW OF CALIBRATION SOURCE

TABLE I. HARMONIC DISTORTION MEASUREMENTS

Chopping Frequency (Hz)	Amplitude (%)		
	1st Harmonic	2nd Harmonic	3rd Harmonic*
20	99	0.7	0.3
33-1/3	99	0.8	0.3
42	99	0.7	0.3
150	99	0.7	0.3
180	99	0.7	0.3
230	99	0.7	0.3
260	99	0.7	0.3

*All other harmonics were of negligible amplitude

Three sources considered for such use were the gallium arsenide photon-emitting diode, the type R1130B Glow modulator tube, and the type A-2 concentrated-arc (zirconium) lamp. Commercially available gallium arsenide diodes are reported to have a flat frequency response extending into the MHz region, a linear transfer function (ratio of output power to input current) over a 10:1 change in input current, and a nearly Lambertian spatial emission pattern [25]. The characteristics of the Glow modulator make this source in general inferior to those of the GaAs diode, but their emission spectra can be the deciding factor: the GaAs diode has only one emission band centered around 0.95μ (fig. 4), whereas the radiation from the Glow modulator tube is distributed in a number of bands located throughout the PbS region (fig. 5). (These spectra were obtained with an interferometer-spectrometer* incorporating an uncooled PbS detector.) Therefore, if the radiometer spectral response precludes the use of the GaAs diode, the Glow modulator can be used. Other available photon-emitting diodes are gallium arsenide-phosphide for the visible region and indium arsenide for around 3.5μ , but these sources are not developed to the present state of the GaAs diodes [26]. Arc instability precluded the use of the zirconium lamp.

3.5. SAMPLE CALIBRATION

In the previous sections, the following parameters were stated to be necessary for specifying the performance of a temporal radiometer: (1) the absolute temporal responsivity, $R(f, \Delta f, \Delta \lambda)$, at one or more frequencies, f_c ; (2) the relative temporal responsivity as a function of frequency throughout the entire range of interest; (3) the responsivity as a function of the amount of incident radiation (i.e., a measurement of both the ac and dc component to check linearity); (4) the relative spatial responsivity; and (5) the relative spectral responsivity.

*Block Model No. 14SF.

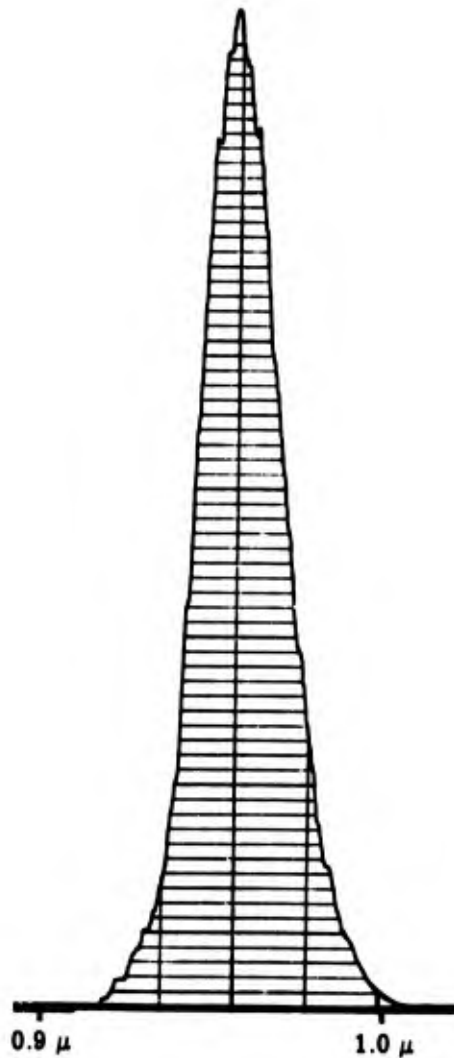


FIGURE 4. RELATIVE GaAs SPECTRUM

The relative spectral responsivity of the temporal radiometer was taken to be the transmittance of the narrow bandpass filter in front of the detector since the change in the spectral response of the detector was assumed to be negligible over this interval. The filter transmittance was measured with a double-beam ratio-recording spectrometer and normalized to a peak value of unity (fig. 6).

The relative spatial responsivity was determined by observing the response of the radiometer to a point source of radiation chopped at 200 Hz. The source was moved in a plane normal to the line of sight and passed through the approximate center of the field of view; the resultant variation is shown in figure 7.

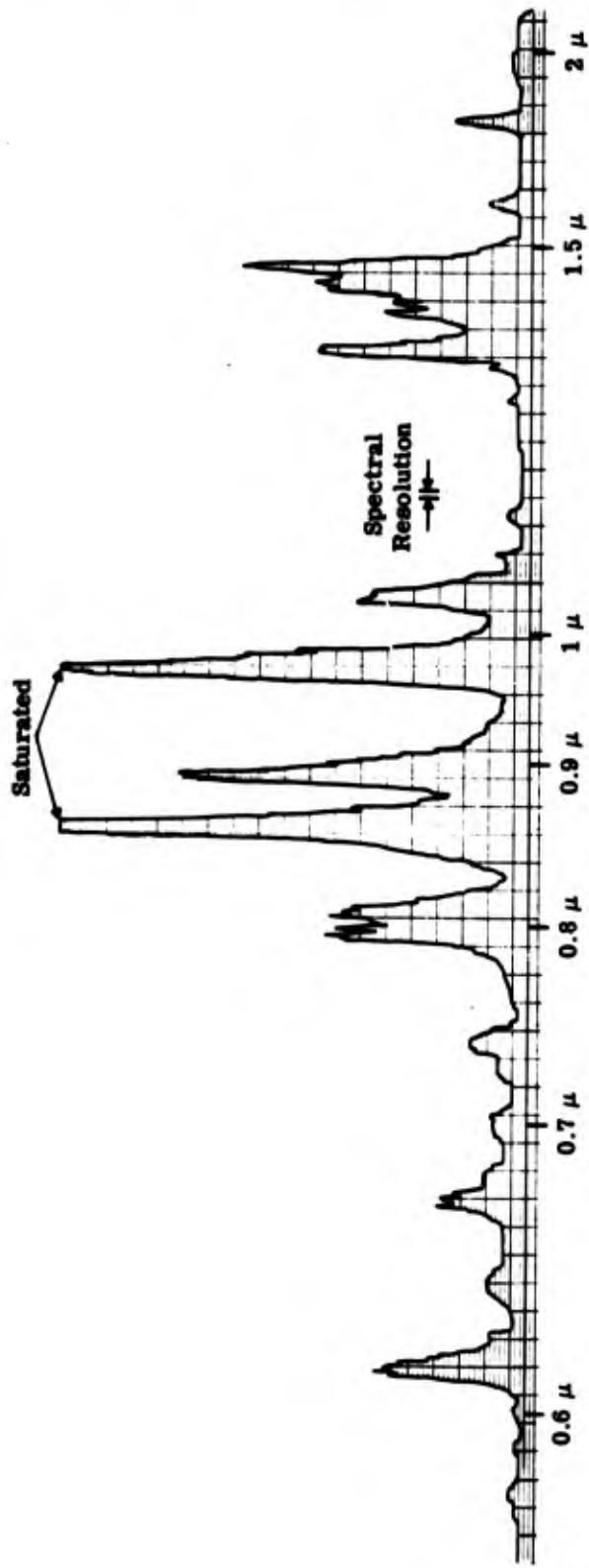


FIGURE 5. RELATIVE GLOW MODULATOR SPECTRUM TYPE R1130B

InSb C0077
18.35 m AWAY (REFOCUSED FOR 18.35 m)

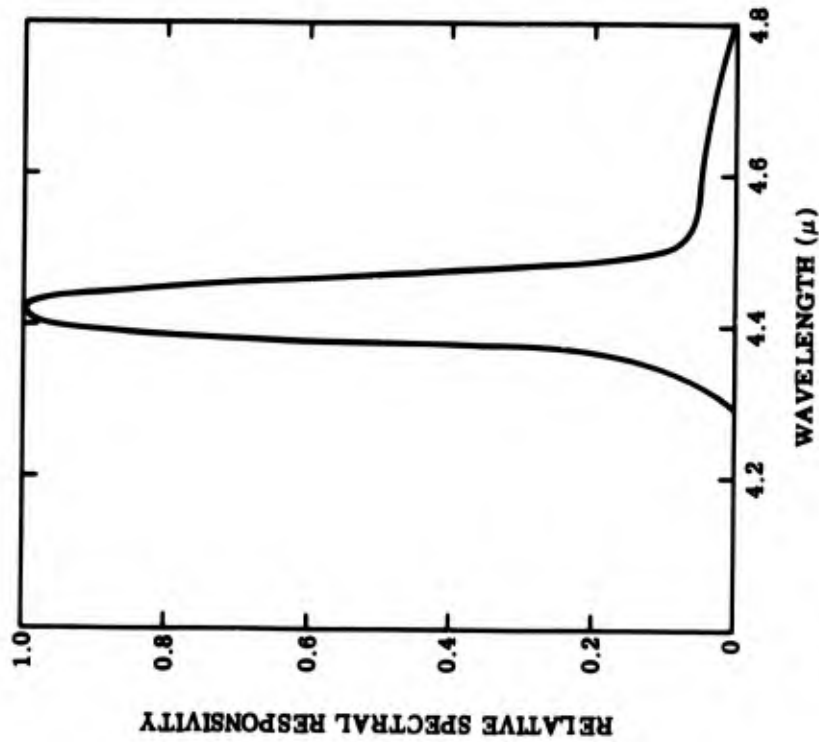
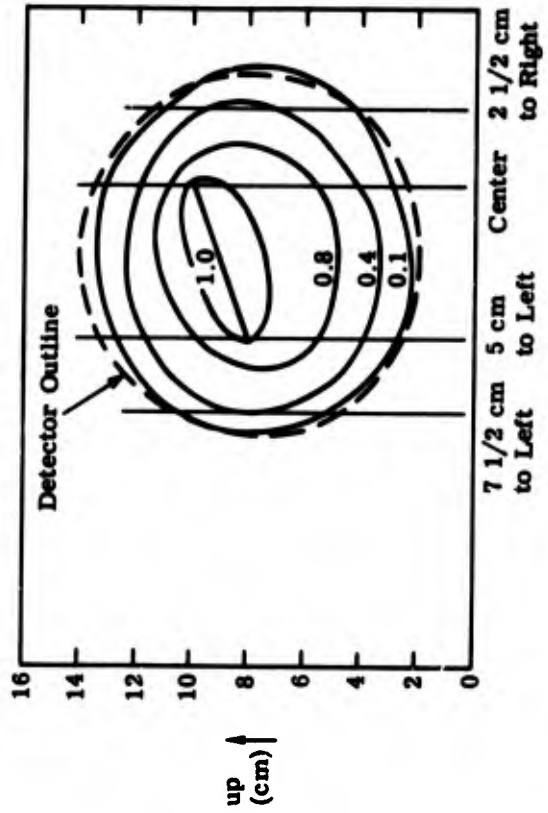
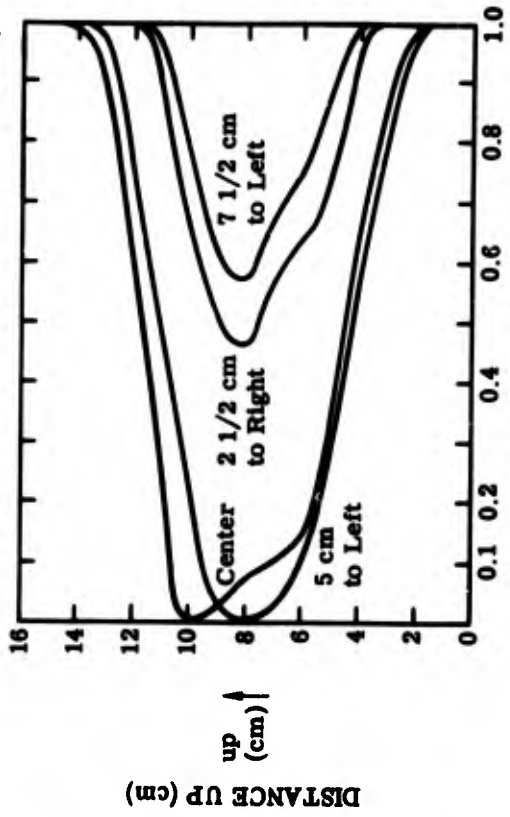


FIGURE 6. RELATIVE SPECTRAL RESPONSIVITY

FIGURE 7. RELATIVE SPATIAL RESPONSIVITY. (a) Temporal radion-
eter field of view; (b) Detector response contours.

The absolute temporal responsivity was measured at a single frequency (750 Hz) over a wide range of irradiance. The blackbody and mechanical chopper were placed a convenient distance from the radiometer aperture to simulate a small source within the field of view. The responsivity was then measured as a function of incident irradiance by adjusting the temperature of the blackbody cavity from 300°C to 600°C in 50° steps. Two different blackbody aperture sizes were used to produce a wider range of irradiance. Responsivities were calculated by use of equation 16. An average transmittance value for the path and wavelength interval involved was computed from [27]. The value was then substituted into equation 16 outside of the integral. The resulting values are shown plotted vs. $\langle H^2(\Delta\lambda) \rangle$ in figure 8. The line drawn through the data points represents the average value, and the amplitude of the vertical "flag" is the standard error.

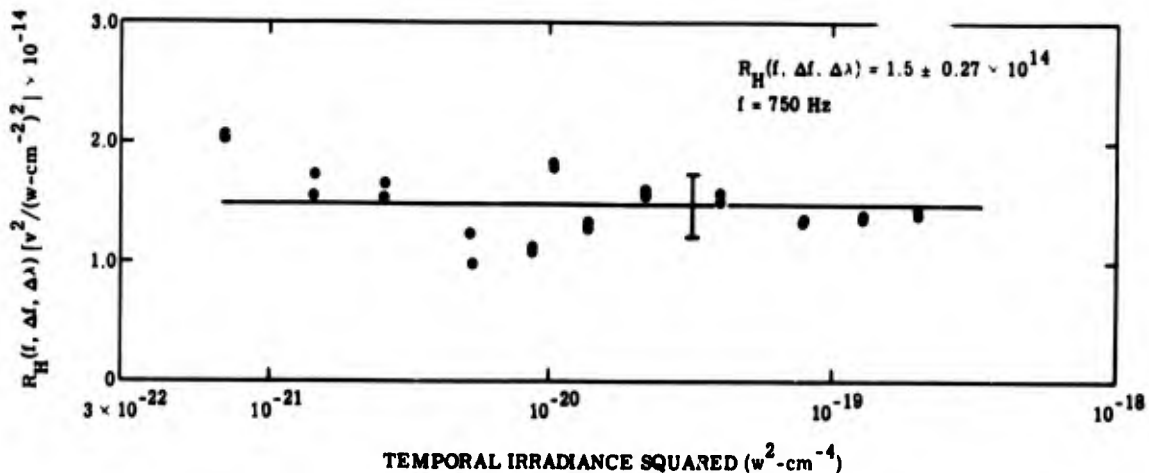


FIGURE 8. TEMPORAL IRRADIANCE RESPONSIVITY

The relative temporal responsivity was measured by illuminating the detector with radiation from a GaAs diode cooled to liquid nitrogen temperature and modulated at audio frequencies with a signal generator. (The relative temporal responsivity for the radiometer system was also determined by measuring the frequency response of each component in the system, preamplifier, tape recorder, and spectrum analyzer separately and computing the composite frequency response. The two methods produced consistent results.) Combining the absolute and relative calibration in equation 17 yields the temporal irradiance responsivity shown in figure 9. The frequency response of the temporal radiometer extends from about 50 Hz to 25 kHz (by the cutoffs of the tape recorder and spectrum analyzer, respectively), but, because the curve is so flat, data are most reliable in the range from 100 Hz to 2 kHz. Furthermore, it is pointed out in appendix II that we have multiple analysis capability in this range.

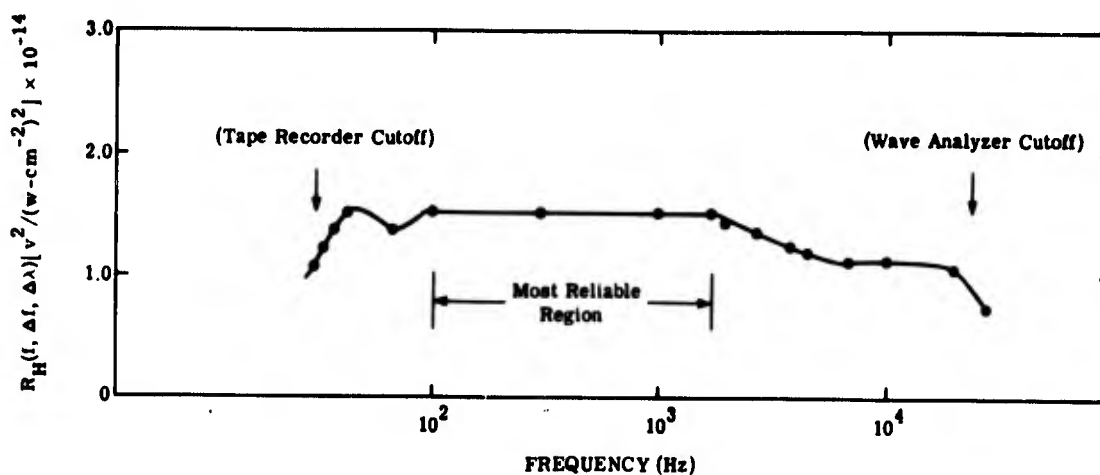


FIGURE 9. TEMPORAL IRRADIANCE RESPONSIVITY AS A FUNCTION OF FREQUENCY

3.6. SQUARE WAVE MODULATED SOURCE CALIBRATION CHECK

The performance of the temporal radiometer was checked by the following procedure. A square wave modulated source was used as a target of known temporal radiance distribution. This source consists of a blackbody (similar to the one described in [28]) located behind a precision chopper and aperture arrangement (fig. 10). The size of the chopper blade and the ratio of chopper spacing to aperture width were made as large as possible in order to approximate square wave modulation. The three-speed synchronous motor provided chopping frequencies of 45, 90, and 180 Hz. The temporal emission characteristics of this unit were compared to those of the temporal radiance standard. Each source was placed an equal distance from the temporal radiometer and set to operate at the same temperature. The cavity temperature of the square wave source was measured with an optical pyrometer (calibrated against an NBS certified tungsten strip lamp). The temporal radiometer contained a filter about 0.1μ wide centered at 2.4μ ; for the path length involved, the atmosphere in this region is essentially 100% transparent [27].

Equation 15 can be written for each source so that, for the temporal standard,

$$R_H(f_1, \Delta f, T, \Delta\lambda) = \frac{\langle P_{f_1}(f_1, \Delta f, T) \rangle \Delta f}{\frac{A_1^2}{8D^4} \left[\int_{\Delta\lambda} N_\lambda \tau(\lambda) S(\lambda) d\lambda \right]^2}$$

where $A_1 = 0.63 \text{ cm}^2$ and $f_1 = 220 \text{ Hz}$; and for the square wave source,

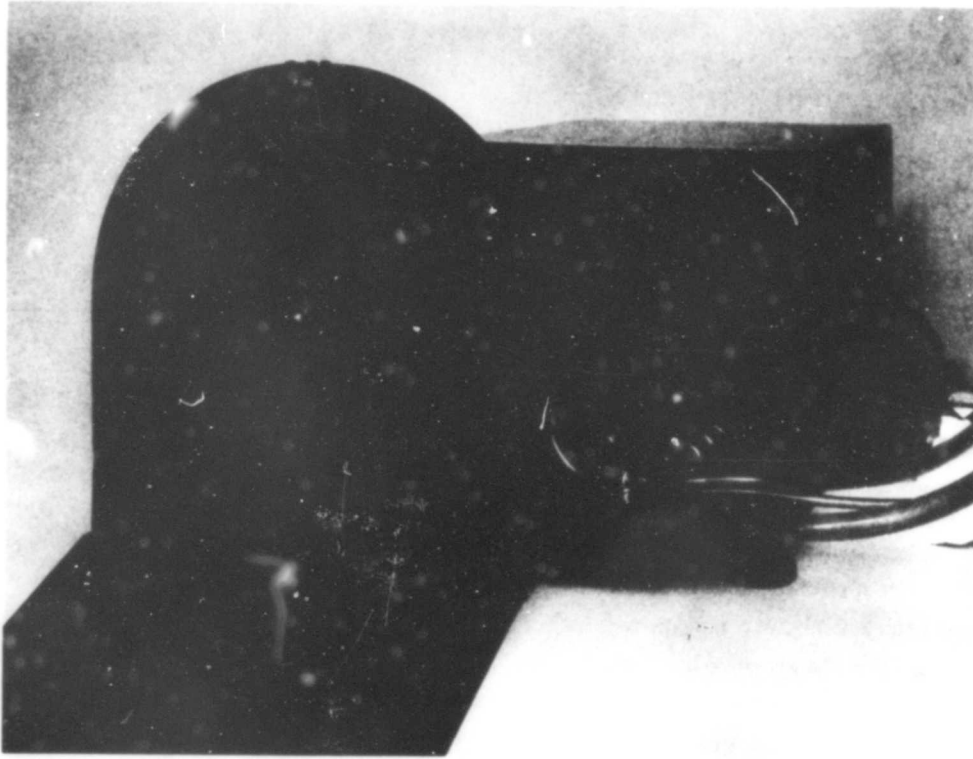


FIGURE 10. PRECISION SQUARE WAVE CHOPPER

$$R_H(f_2, \Delta f, T, \Delta\lambda) = \frac{\langle P_{f_2}(f_2, \Delta f, T) \rangle \Delta f}{\frac{\pi^2 A_2^2}{32D^4} \left[\int_{\Delta\lambda} N_\lambda \tau(\lambda) s(\lambda) d\lambda \right]^2}$$

where $A_2 = 0.184 \text{ cm}^2$ and $f_2 = 180 \text{ Hz}$ is the square wave fundamental or chopping frequency. Equating the responsivities,*

$$\frac{\langle P_{f_1}(f_1, \Delta f, T) \rangle \Delta f}{\frac{A_1^2}{8D^4} \left[\int_{\Delta\lambda} N_\lambda \tau(\lambda) s(\lambda) d\lambda \right]^2} = \frac{\langle P_{f_2}(f_2, \Delta f, T) \rangle \Delta f}{\frac{\pi^2 A_2^2}{32D^4} \left[\int_{\Delta\lambda} N_\lambda \tau(\lambda) s(\lambda) d\lambda \right]^2} \quad (20)$$

*No correction is needed because the chopping frequencies f_1 and f_2 are different. If figure 9 is correct, both lie on the flat part of the response curve.

WILLOW RUN LABORATORIES

Eliminating common variables,

$$\frac{\langle P_{f_1}(f_1, \Delta f, T) \rangle}{A_1^2} = \frac{\langle P_{f_2}(f_2, \Delta f, T) \rangle}{(\pi^2 A_2^2)/4}$$

Taking the square root of both sides and rearranging yields

$$\left[\frac{\langle P_{f_2}(f_2, \Delta f, T) \rangle}{\langle P_{f_1}(f_1, \Delta f, T) \rangle} \right]^{1/2} = \frac{\pi A_2}{2A_1} = 0.458 \quad (21)$$

where subscripts 1 and 2 refer to sine wave and square wave, respectively. Two independent experimental measurements of P_{f_1} and P_{f_2} produced the ratios 0.451 and 0.464, which agree with the predicted value within the experimental error. This establishes that the temporal responsivity calibration is valid for at least the first harmonic of a periodic signal.

Next, the harmonic content of the square wave source was analyzed for each of the three fundamental frequencies. Figure 11 is an amplitude spectrum for the 45-Hz square wave; the 20-Hz filter was used. The signal at 0 Hz represents the local oscillator.

For the 180-Hz chopping frequency, table II gives an analysis of the frequency content found experimentally and derived theoretically. The correction factors were obtained from figure 9. The theoretical values included the proper slope in the sides of the square wave as determined from the geometry of the aperture and chopper. Above the third harmonic, considerable disagreement was noted between the two values. This may be due in part to less-than-perfect imaging of the aperture shape on the detector. However, the amplitudes of these higher harmonics are small, compared to the fundamental, so that the percent error is within that expected for the available signal and noise levels.

TABLE II. ANALYSIS OF 180-Hz SQUARE WAVE

Frequency (Hz)	Relative Fourier Amplitudes		
	Experimental*	Theoretical	% Error
180	1.0	1.0	0
540	0.335	0.332	0.9
900	0.188	0.199	5.5
1260	0.125	0.142	12
1620	0.09	0.111	19
1800	0.063	0.093	32
1980	0.052	0.076	31

*Including calibration factors

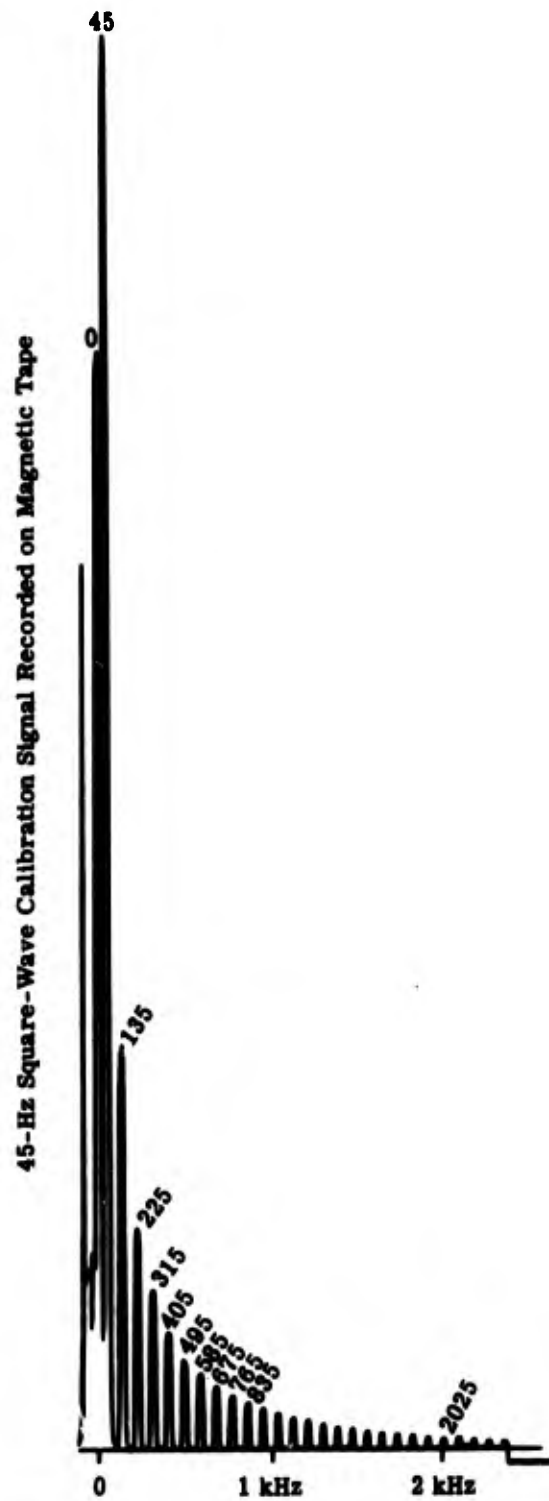


FIGURE 11. SAMPLE DATA-FREQUENCY ANALYSIS OF 45-Hz SQUARE WAVE

SUMMARY AND CONCLUSION

A frequency distribution was sought of a quantity ψ_f such that

$$\psi(\Delta\lambda, \Delta f) = \int_{f_1}^{f_2} \psi_f df \quad (1)$$

where $\psi(\Delta\lambda, \Delta f)$ is a quantity related to the time-varying irradiance at the entrance aperture of the radiometer in the spectral interval $\Delta\lambda$ and the modulation interval $\Delta f = f_2 - f_1$. When the principles of electrical noise theory were applied to radiometry, it was indicated that a good measure of the time-varying irradiance is provided by the mean square irradiance (or rms irradiance) for periodic signals. Also, a measure for randomly varying irradiances was provided by the mean square irradiance density. Thus, for periodic signals,

$$\langle H^2(f, \Delta\lambda) \rangle = \frac{\langle P_f(f, \Delta f, T, \Delta\lambda) \rangle \Delta f}{R_H(f)} = \frac{P}{R_H(f)} \quad [(w\text{-cm}^{-2})^2] \quad (22)$$

where P = electrical power (v^2)

R_H = temporal irradiance responsivity [$v^2/(w\text{-cm}^{-2})^2$]

For random signals:

$$\frac{\partial H^2}{\partial f} \equiv \langle H_f^2(f, \Delta f, T, \Delta\lambda) \rangle = \frac{\langle P_f(f, \Delta f, T, \Delta\lambda) \rangle}{R_H(f)} \quad [(w\text{-cm}^{-2})^2\text{-Hz}^{-1}]$$

Thus we could generalize to:

$$\psi_f(f) \equiv \frac{\partial H^2}{\partial f} \equiv \frac{P_f(f)}{R_H(f)} \quad [(w\text{-cm}^{-2})^2\text{-Hz}^{-1}]$$

where $P_f(f)$ is the power spectral density function in units of $v^2\text{-Hz}^{-1}$, and $R_H(f)$ is the mean square responsivity or "temporal responsivity" in units of $v^2/(w\text{-cm}^{-2})^2$.

In the special case of periodic signals, P_f reduces to

$$P_f(f_0) = \delta(f - f_0)P$$

where P = electrical power, which in this case is a constant independent of bandwidth.

Based on the method of data analysis, a calibration technique was developed, employing blackbody radiation sinusoidally modulated with a mechanical chopper. In order to cover the frequency range of the radiometer, the "temporal radiance standard" was augmented with a

WILLOW RUN LABORATORIES

gallium arsenide photon-emitting diode modulated by an audio oscillator. The remainder of the calibration was in keeping with standard radiometric practices [22, 23], except that all sources were modulated. The final step was to check the performance of the calibrated temporal radiometer against a known "unknown" source, which was a square wave modulated blackbody. Agreement was found within the experimental error due to the available signal and noise levels.

Thus, a single calibration technique for temporal radiometers was developed which allows for the quantitative treatment of both periodic and statistically fluctuating sources of optical radiant energy.

**Appendix I
INSTRUMENTATION**

I.1. RADIOMETERS

Two radiometers, one for measuring the temporal fluctuations and the other for measuring the time-averaged signal, were fabricated for this study. Each instrument (fig. 12) consists of a photovoltaic InSb detector about 2.5 mm in diameter mounted in the focal plane of a Dahl-Kirkhan optical system behind a narrowband filter (4.45-4.55 μ). The primary mirror diameter is 5.875 in., the secondary mirror diameter 2.85 in., and the focal length is 15 in. The detector voltage in each radiometer is amplified in a high-gain (≈ 750) wide-bandwidth (5-200kHz) preamplifier to a suitable level. The signal from the temporal radiometer was recorded on magnetic tape while being monitored on an oscilloscope. The other radiometer contained a chopper operating at 90 Hz, the amplified signal of which was synchronously rectified. The resultant dc level was displayed on a chart recorder.

I.2. ELECTRONICS

The system (fig. 13) is assembled in four rack panels, 19-in. wide and 61-in. high, with attached table. Only the magnetic tape recorder and the wave analyzer are described in detail, because the other components are used in their normal mode. The method used to adapt the magnetic tape recorder to continuous-loop playback is believed sufficiently unusual to warrant a discussion.

I.2.1. TAPE RECORDER. Since an analog method of data reduction and analysis was selected, it was necessary to obtain a magnetic tape recorder with a continuous or closed-loop playback capability. Other desired features for the tape recorder were that the unit (a) be portable for field measurements, (b) be of reasonable instrumentation quality, (c) have a minimum of four data channels, and (d) use 1/4-in. tape. To meet these requirements, the 4-channel, Ampex Model SP-300 recorder was selected. As supplied by the manufacturer, this recorder has direct and FM record and playback capability at speeds of 1 7/8 through 15 ips.

Before the present continuous-loop playback system was perfected, measurements were attempted on a system involving the suspension of the magnetic-tape loop on four stationary aluminum tape guides rotating on ball-bearing mounts, and a fifth movable guide weighted to give approximately the correct tension on the tape. An analysis of this playback method indicated that the tension on the tape differed sufficiently from the data recording mode to introduce a gain change of about 2 db. Also, it was learned that the signal level changes during playback by about 1 1/2 db from beginning to end of a 10 1/2-inch reel of tape for a recorded signal con-

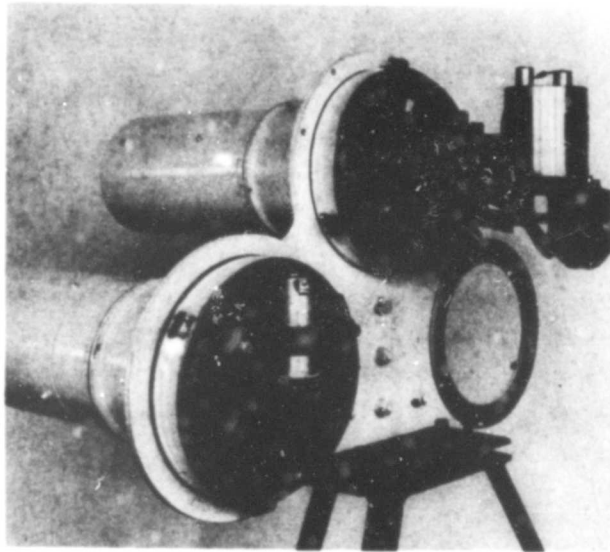


FIGURE 12. RADIOMETERS WITHOUT REAR COVERS

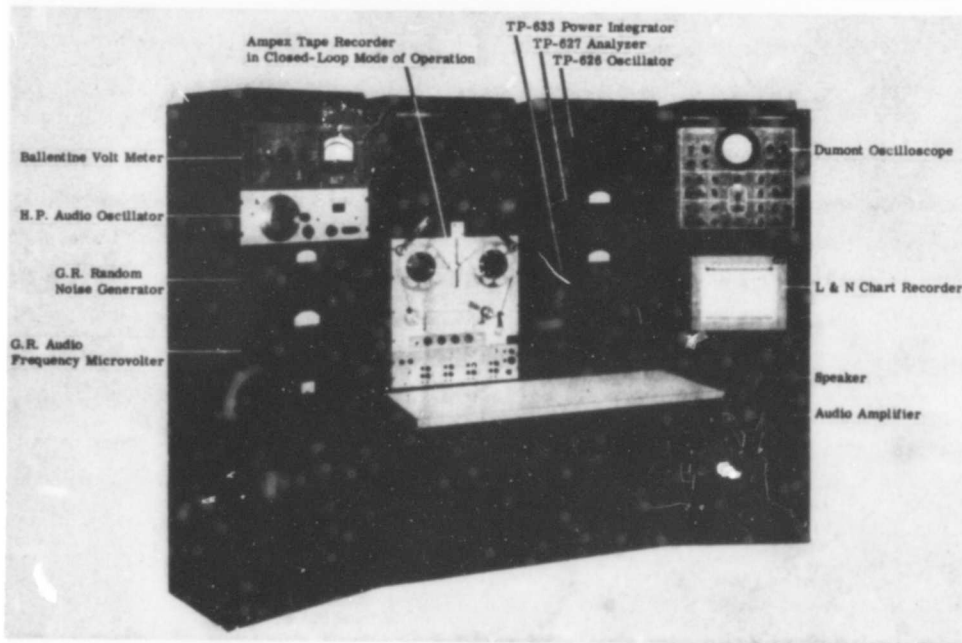


FIGURE 13. CONTINUOUS-LOOP PLAYBACK SYSTEM

stant to within 0.1 db. A continuous-loop playback system which relied upon the machine itself to achieve the proper tape tension was then constructed and found to be more satisfactory. This system is shown in figure 13. Two aluminum hubs 6 1/2 in. in diameter (the mean diameter of a 10 1/2 inch reel of magnetic tape) replace the normal magnetic-tape reels. Each aluminum hub has a 1/8 x 1/4-in. groove around the outer edge to act as a guide for the magnetic tape. The grooves are lightly sand-blasted to achieve the required friction so that tape slippage will not occur. Rubber-covered ball bearings that ride within each 1/8 x 1/4 groove are attached to the spring-loaded aluminum arms. These arms are mounted in a piece of 1/2-in.-thick aluminum tooling plate mounted in the rack panel above the tape recorder. By clamping the magnetic tape (in closed-loop form) between the rubber-covered ball bearing and the aluminum hub, the same tape tension is achieved in closed-loop operation as during the reel-to-reel recording of the data. The small aluminum roller located between the two 6 1/2-in.-diameter hubs acts only to guide the tape from one hub to the other and prevents static electricity from interrupting the playback. Over 100 hr of operation have been put on this closed-loop playback system with no observable deterioration in any of the tapes or the components. The performance of the machine in the closed-loop playback mode was shown by measurements to be equal to that of the machine in the reel-to-reel mode. Another virtue of this method of closed-loop playback is that the tape loop has the shortest possible recirculating time. Extensive modifications of the tape-transport plate leading to smaller closed loops were not considered practical because the reel-to-reel capability of the machine had to be retained.

I.2.2. WAVE ANALYZER. The spectrum analyzer selected for the project consists of three subunits: a tunable oscillator, a heterodyne type analyzer, and a power integrator, Models TP-626, TP-627 and TP-633, respectively, manufactured by Technical Products, Inc., Los Angeles, California. The proper operation of the analyzer in the power spectrum mode is discussed in appendixes II and III.

Appendix II PRACTICAL ASPECTS OF POWER SPECTRAL DENSITY ANALYSIS

II.1. INTRODUCTION

This appendix covers the application of power spectral density analysis to random IR signals. That is, given the selected parameters of filter bandwidth, scan rate, data sample length, and averaging time, we wish to determine the proper adjustment which will satisfy specified requirements of accuracy and resolution. In order to obtain optimum results, this process may

involve some "feedback"; i.e., we initially set up some requirements of accuracy and resolution which can later be made more or less stringent, depending upon the outcome.

II.2. RELATION OF THEORY TO ANALYZER OPERATIONS

Given a stationary* random signal $y(t)$ of length T sec, the power spectral density function $P_f(f)$ is defined as

$$P_f(f) = \lim_{T \rightarrow \infty} \lim_{\Delta f \rightarrow 0} \frac{1}{T \Delta f} \int_0^T y_{\Delta f}^2(t) dt \quad (23)$$

where $y_{\Delta f}^2(t)$ is the square of the instantaneous amplitudes within the narrow frequency interval f and $f + \Delta f$, and T is the integration time.

Figure 14 represents a possible power spectrum (i.e., a plot of the power spectral density, sometimes abbreviated PSD) function $\langle P_f(f, \Delta f, T) \rangle$ versus frequency. The area under the PSD curve between any two frequencies f_1 and f_2 is equal to the mean square value of the signal within that frequency range.

Figure 15 is a functional block diagram illustrating the wave analyzer's operation in the power spectrum mode. A glance at the diagram indicates that there are only two modifications to the standard heterodyne process. First, the rectification is performed by a square-law circuit rather than being the usual linear rectification; and second, provision is made for division by the filter bandwidth Δf .

The squaring circuit consists of a nonlinear amplifier and filter with an input-output relationship that can be expressed as a power series. For this particular unit, the plate voltage and the bias voltage are set so that the squared term predominates. With the aid of the filter, only the squared term is passed to the averaging circuits.

The division by bandwidth is performed by a variable resistor which is carefully calibrated to attenuate the signal by the noise equivalent bandwidth (see app. III).

Thus the output on the L&N chart recorder is a direct estimate of the power spectrum, $\langle P_f(f, \Delta f, T) \rangle$ vs. f . Of course, since the analyzer cannot perform a limiting process, the degree to which the PSD estimate agrees with the true value depends upon the choice of integration time and bandwidth.

*A signal such that averages, when performed on successive samples, show no trend to change with time. In practice, the fluctuations are usually not stationary, but are approximately so for short intervals. Stationarity is assumed as long as the dc level is constant.

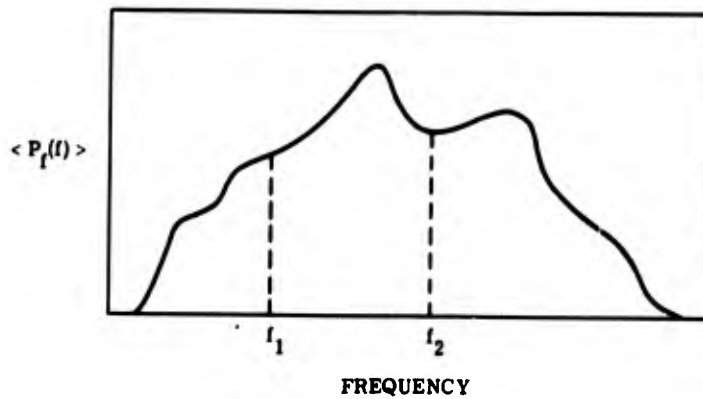


FIGURE 14. TYPICAL POWER SPECTRUM

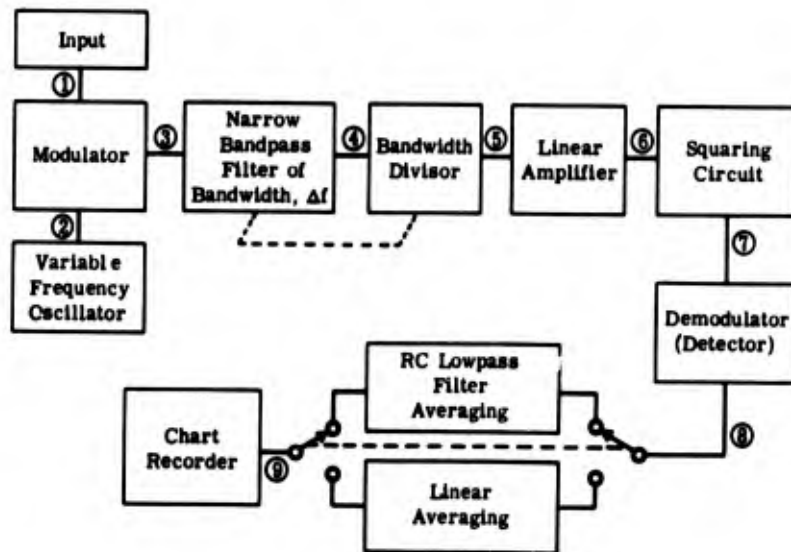


FIGURE 15. SPECTRUM ANALYZER BLOCK DIAGRAM

II.3. ANALYSIS ACCURACY

The analysis of random data involves not only basic measurement errors, but also statistical limitation inherent in sampling procedures [29-32]. As implied above, the meaning of the analysis will depend upon how well $\langle P_f(f, \Delta f, T) \rangle$ estimates the true PSD function, $P_f(f)$. The statistical parameters which define the accuracy of the estimation are: degrees of freedom, uncertainty, and confidence level; the relation between the three is illustrated in a chi-square distribution chart (fig. 16). The ordinate of the chart is the ratio of $\langle P_f(f, \Delta f, T) \rangle$ to $P_f(f)$; the abscissa is degrees of freedom, and the parameters are confidence bands.

Degrees of freedom indicate the ratio of the mean square fluctuation of a variable to the true squared average and is given by [19, 20]

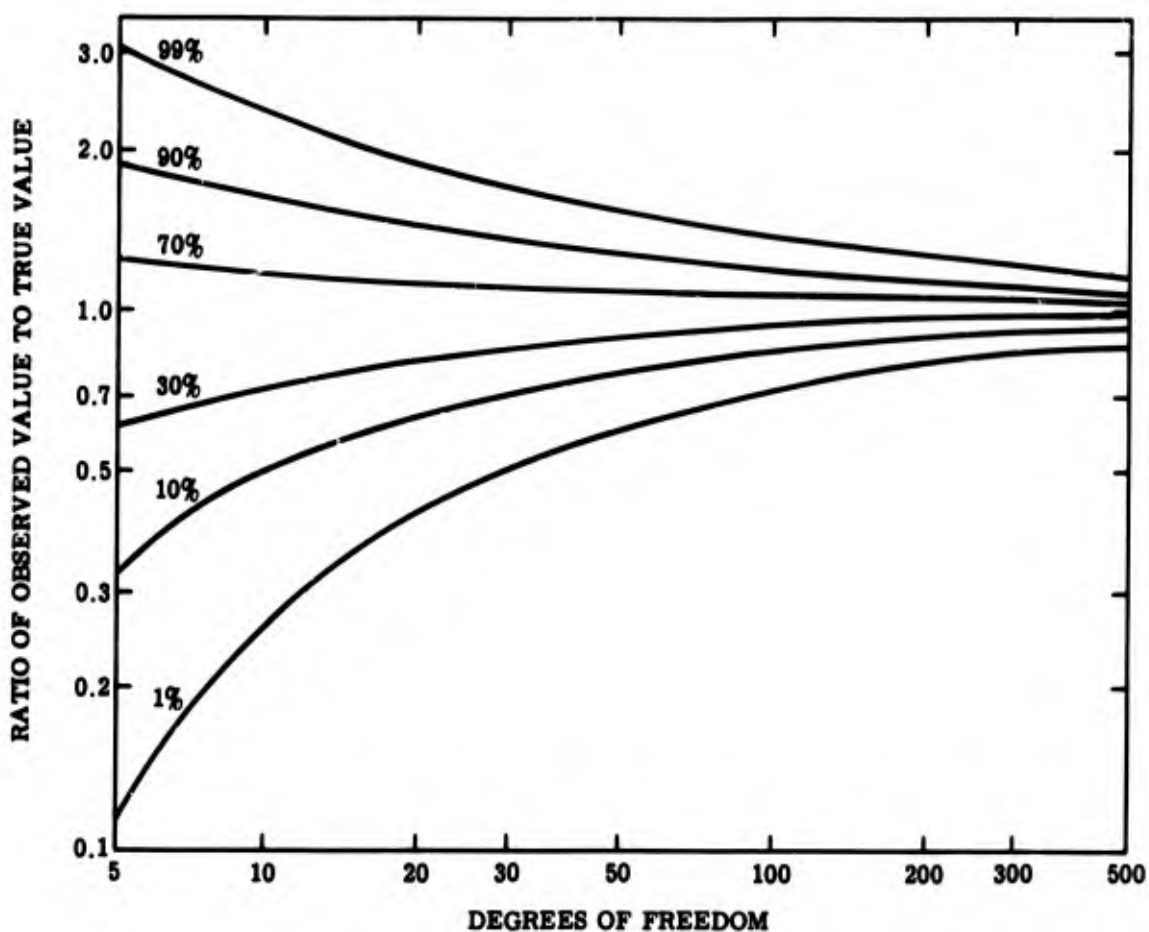


FIGURE 16. CHI SQUARE DISTRIBUTION CHART [19]

$$N = 2T_d \Delta f \quad (24)$$

where N = degrees of freedom

Δf = bandwidth of selective filter in spectrum analyzer (Hz)

T_d = data sample length (sec)

The larger the product $2T_d \Delta f$, the more accurately known $P_f(f)$ is. (This explains the notation $T \Delta f \rightarrow \infty$ in eq. 23.) A value of 100 has been selected as a reasonable value for N . As seen in the chi-square chart (fig. 16), for values higher than 100 the confidence level does not increase appreciably; for values much lower than 100 the confidence level decreases quite rapidly.

As an example, suppose we have a filter whose bandwidth Δf is 20 Hz and a data sample length T_d of 2 1/2 sec.* Then $N = 100$ degrees of freedom. From the chart we see that there is a 99% confidence that the estimate will be above $0.72P_f(f)$ of the true value and a 1% confidence that it will be above $1.30P_f(f)$. Thus we have 98% confidence that observed value will fall between 0.72 and 1.30 of the true value of the function, or

$$P_f(f) \cong (1 \pm 0.3) \langle P_f(f, \Delta f, T) \rangle \quad (25)$$

about 98% of the time (100 degrees of freedom). Note that once the degrees of freedom are specified, uncertainty and confidence become directly related; i.e., the uncertainty can only be decreased at the sacrifice of confidence in the estimate.

The statistical uncertainty is often expressed in terms of the standard error σ . For the specific case of power spectral density analysis, the standard error associated with a measured estimate $\langle P_f(f, \Delta f, T) \rangle$ is [29, 30]

$$\sigma = \frac{1}{\sqrt{T_d \Delta f}}, \text{ for } \sigma \leq 0.20 \quad (26)$$

where Δf is the noise bandwidth[†] of the selective filter in Hertz and T_d is the length of the analyzed sample record in seconds. Thus if an estimate $\langle P_f(f, \Delta f, T) \rangle$ is measured from a data sample, it may be said that the true value

$$P_f(f) \cong (1 \pm \sigma) \langle P_f(f, \Delta f, T) \rangle \quad [68\% \text{ confidence}] \quad (27)$$

For example, let a measured estimate $\langle P_f(f, \Delta f, T) \rangle$ at a given frequency be $0.5 \text{ v}^2/\text{Hz}$, the sample length be $T = 2.5$ sec, and the filter bandwidth Δf be 20 Hz; then $\sigma \cong 0.14$ and it may be said with about 68% confidence that the true power spectral density function for that frequency is $P_f(f) = (1 \pm 0.14) \langle P_f(f, \Delta f, T) \rangle$; i.e., 68% of the time the true PSD function will be between 0.43 and $0.57 \text{ v}^2/\text{Hz}$.

II.4. RESOLUTION[‡]

We have seen (eq. 26) that the statistical uncertainty of power spectral density estimates is inversely proportional to the bandwidth of the analyzer filter: increasing the bandwidth reduces the uncertainty. However, increasing the filter bandwidth reduces the resolution of the

*The integration time is set to equal the data sample length.

†See appendix III for a definition and measurement of noise bandwidth of a filter, and its effect on proper PSD measurements.

‡Sections II.4 to II.7, which present the generally accepted criteria or "rules of thumb" for selection analysis parameters, rely heavily on reference [31].

analysis; i.e., it reduces the ability of the analysis to properly define sharp peaks in the power spectrum. So the selection of the analyzer filter bandwidth is always a compromise between estimation uncertainty and resolution. Further, if there are sharp peaks within the filter bandwidth, the statistical uncertainty will actually be increased. Hence, the emphasis should be placed upon an analyzer bandwidth which will give proper resolution. A reasonable criterion for proper resolution is a filter bandwidth that is one-fourth the bandwidth (between half-power points) of the narrowest peak in the power spectrum, or

$$\Delta f < 0.25(f_2 - f_1) \tag{28}$$

where Δf is the analyzer filter bandwidth and $(f_2 - f_1)$ is the bandwidth between half-power points of a PSD peak, both in Hertz. Note that, for spectral peaks with relatively low center frequencies, say less than 50 Hz, a peak or prominence in the power spectrum may have a bandwidth of less than 1 Hz, thus requiring a filter bandwidth on the order of 0.25 Hz. Since the narrowest filter bandwidth available for the spectrum analyzer is about 2 Hz, the required resolution would not ordinarily be possible. One way to circumvent this problem is to play the data back faster than it was recorded, since this effectively reduces the bandwidth by an amount equal to the tape speedup factor.*

II.5. SAMPLE RECORD LENGTH

As seen from equation 24, the sample length T is one factor that limits the statistical accuracy attainable in a PSD estimate. Limiting the statistical uncertainty of a PSD analysis to a given desired amount must therefore be considered before the data are gathered to assure that sample records are sufficiently long.

II.6. AVERAGING TIME

The mean square amplitude detector incorporated in a PSD analyzer computes a mean square value by averaging the instantaneous output of a square-law rectifier. Either true linear integration or continuous smoothing with an equivalent lowpass RC filter may do the averaging; PSD analyzers are usually equipped with both types of averaging circuits. True averaging produces a single PSD estimate after a specific averaging time interval T_a , whereas RC averaging produces a continuous PSD estimate.

The general criterion for the averaging time for a PSD analysis is

$$\text{for true averaging} \quad T_a = T_d \tag{29a}$$

$$\text{for RC averaging} \quad K \geq T_d \tag{29b}$$

*The advantages of tape speedup are discussed in references 29 and 30.

where T_a is the true integrating time, K is the time constant of the equivalent RC averaging time, and T_d is the data sample length, all in seconds.

II.7. SCAN RATE AND ANALYSIS TIME

For a single-filter heterodyne-type analyzer, the PSD is analyzed by scanning through the desired frequency range. If the scan rate is too fast, the statistical uncertainty of the resulting estimate will be increased because all the information available at a given frequency will not be viewed by the analyzer filter over the entire record length. The limitations imposed upon the scan rate by this consideration follow.

Let the scan rate be denoted by r ; then for true averaging,

$$r \cong \left. \begin{array}{l} \Delta f / T_a \\ \Delta f^2 / 8 \end{array} \right\} \quad (30a)$$

whichever value gives the slower scan rate; and for RC averaging,

$$r \cong \left. \begin{array}{l} \Delta f / 4K \\ \Delta f^2 / 8 \end{array} \right\} \quad (30b)$$

whichever values gives the slower scan rate. The scan rate unit is Hertz per second. The analysis time τ may be defined as

$$\tau \equiv \frac{\text{frequency range scanned}}{\text{scan rate}} = \frac{f_2 - f_1}{r} \quad [\text{sec}] \quad (31)$$

II.8. EXAMPLE

We now wish to illustrate the procedure for making a reasonable PSD estimate over the audio frequency range of the IR radiation from some target. The output of the temporal radiometer can be recorded on two channels, one on FM for the low-frequency response (0-50 Hz), and one on "direct" for high-frequency response (50-25,000 Hz). This requires two analyses, one for each channel of data. Let us assume that the samples of stationary data are short, say $T = 4$ sec, and that we require a standard error of 0.15 or less; i.e., $P_f(f) \leq (1 \pm 0.15) \langle P_f(f) \rangle$ over the entire spectrum. Table III is a list of filter bandwidths, averaging time, scan rates, and other pertinent parameters of the spectrum analyzer at our disposal. We should like to choose the proper combination of these parameters, consistent with the above restrictions and our previously stated criteria, to minimize analysis time. Hence, a crude "quick-look" scan of the spectrum is advisable in order to establish the approximate location and bandwidth of any prominences. As pointed out in [20], we generally expect sharp prominences at low (0-50 Hz)

WILLOW RUN LABORATORIES

TABLE III. PARAMETERS FOR DATA REDUCTION SYSTEM

Filters

RC averaging time constant: $0.1 \leq K \leq 100$ sec, continuously adjustable

Filter No.	Nominal Bandwidth (Hz)	Noise Equivalent Square Bandwidth (Hz)
1	2	2.88
2	20	24.5
3	200	206.4

Scan Rates (Hz-sec⁻¹)

Closed loop length: $L \geq 53$ in. or 3.5 sec at 15 ips

Scan Rate	Frequency Scale		
	$\times 1$ Range 0-250 Hz	$\times 10$ Range 0-2500 Hz	$\times 100$ Range 0-25,000 Hz
Fast	0.48	4.8	48
Slow	0.048	0.48	4.8

Tape Recorder Frequency Response
(From Ampex Manual)

Record/Playback Speeds (ips)	Direct Mode	FM Mode
1 7/8	(50-5k Hz) \pm 3 db	0-312 Hz
3 3/4	(50-10k Hz) \pm 3 db	0-625 Hz
7 1/2	(50-20k Hz) \pm 3 db	0-1250 Hz
15	(50-40k Hz) \pm 3 db	0-2500 Hz

frequencies, and wider, smoother prominences at higher frequencies. As a realistic example therefore, let us suppose that our "quick-look" scan has revealed several very sharp prominences (halfwidth \sim 2 Hz) below 50 Hz, some less sharp prominences (halfwidth \sim 100 Hz) in the range (50-2500) Hz, and a relatively smooth spectrum above 2500 Hz.

Consider first the resolution requirements on our filter bandwidth (eq. 28). In the low-frequency range, we need a bandwidth of approximately 0.5 Hz for proper resolution. But from the initial conditions,

$$\frac{1}{\sqrt{4(\Delta f)}} = \sigma \leq 0.15$$

which imposes the condition that

$$\Delta f \geq 20 \text{ Hz}$$

it is clear that any prominence in the spectrum of a bandwidth less than approximately 80 Hz cannot be properly resolved with any reasonable statistical confidence. Therefore, we would not bother to analyze the range 0-50 Hz since the shortness of data sample and the available resolution cannot yield significant results.*

For the higher frequencies (1000-25,000 Hz), the quick-look scan indicated a smooth spectrum. In this range we may use a wide filter (200 Hz) since our resolution criteria impose no restriction. The standard error will then be $\sigma \cong 0.04$; i.e., a highly precise estimate of $P_f(f)$ will be generated. We need a scan rate of

$$r \leq \frac{\Delta f}{4K} = \frac{200}{16} = 12.5 \text{ Hz-sec}^{-1}$$

i.e., the scan rate must not be greater than 12.5 Hz-sec^{-1} , and an RC-averaging time[†] of $K = 4 \text{ sec}$. In table III we have an available scan rate on the $\times 100$ scale (0-25,000 Hz) of 5 Hz-sec^{-1} , so that the analysis time for this frequency range is

$$\tau = 24,000/5 = 4800 \text{ sec}$$

or approximately 1 hr, 20 min.

We can reduce the analysis time (with a corresponding loss in precision) by reducing the averaging time. If we let $K = 1 \text{ sec}$ and $\Delta f = 200 \text{ Hz}$, the scan rate is 50 Hz-sec^{-1} (which can be handled by FAST SPEED scan), and the precision becomes

$$\sigma = \frac{1}{\sqrt{200(1)}} = 0.07 \quad \text{or} \quad P_f(f) = (1 \pm 0.07) \langle P_f(f, \Delta f, T) \rangle$$

which has twice the precision of our minimum requirements. The analysis time is reduced to 8 min, a very considerable saving, but of course, this is based on the premise of a smooth spectral region. Note that no further reduction in analysis time is possible, since this is our fastest scan rate; i.e., we have optimized this part of the analysis for our equipment.

This leaves for our consideration the range (50-1000 Hz), where we must resolve prominences on the order of 100 Hz. Our 20-Hz filter fits this resolution requirement very well. With $K = T = 4 \text{ sec}$, σ becomes 0.15 (our minimum requirement), and the required scan rate is

*There is however the possibility of "pooled estimates"; see reference 20 for a discussion of this technique of analysis.

† We presume that a continuous estimate of PSD is desired.

1.25 Hz-sec⁻¹. Our closest available scan rate is 0.48 Hz-sec⁻¹, so that the analysis time will be about 30 min. Had the maximum scan rate been available, the analysis would have taken only 16 min. The TP-625 wave analyzer has an optional accessory which provides continuously variable scan rates. If absolute minimum analysis time were a requirement, such a device would be very attractive.

It may turn out that in the lower portion of the spectrum (50-2500 Hz) the 20-Hz filter will not give acceptable resolution. Our only recourse is to employ the 2-Hz filter, which will resolve PSD prominences whose bandwidth is 8 Hz or greater, with a corresponding loss in statistical confidence.* If we then set K = 4 sec, the required scan rate is 0.125 Hz-sec⁻¹, which can be accommodated in the 50-250-Hz range by our SLOW scan rate of 0.048 Hz-sec⁻¹. The analysis time would be about 70 min. By comparing this analysis with the previous one, it should be possible to obtain a reasonable estimate of the PSD function in this range, i.e., a "pooled estimate."

Summarizing the procedure for this example: a quick-look scan was made to help determine the proper combination(s) of filter bandwidth, averaging time, and scan rate to minimize analysis time. The lower frequency range (0-50 Hz) was not analyzed because of shortness of data sample length and lack of resolution. The upper frequency range (2500-25,000 Hz) was analyzed in 8 min; the range 50-2500 Hz was analyzed in 30 min; and the range 50-250 Hz was reanalyzed with greater resolution in 70 min; the total analysis time was thus 1 hr, 48 min. Had a variable-scan-rate accessory been available to optimize the scan rate, approximately 1 hr could have been eliminated from this total.

Appendix III CALIBRATION OF SPECTRUM ANALYZER FOR DIRECT POWER SPECTRAL DENSITY MEASUREMENTS

III.1. DEFINITION OF NOISE BANDWIDTH

In PSD measurements, it is necessary to know the noise bandwidth Δf of the frequency selective filter in the spectrum analyzer. An "ideal" filter has a flat top and vertical skirts, whereas practical filters depart somewhat from this design. Any filter when driven by a generator of white random noise will deliver an output power (voltage squared) proportional to its

*Note that the standard error formula $\sigma = 1/\sqrt{T \Delta f}$ is not valid for $\sigma \geq 0.20$, so that we must use the chi-square distribution chart and the degrees of freedom $N = 2T \Delta f$. In this case $N = 2(2)(4) = 16$ degrees of freedom. From figure 16 we see that the true PSD function $P_f(f)$ will lie between $0.6 < P_f(f, \Delta f, T) >$ and $1.2 < P_f(f, \Delta f, T) >$ about 60% of the time in the long run (a statistical confidence of 60%).

bandwidth. Now, suppose a practical filter has an output power P . Then the noise bandwidth, or effective bandwidth, is defined as the bandwidth of an ideal filter producing the same output power; i.e.,

$$P = \frac{1}{\Delta f} \int_{f_1}^{f_2} E^2(f)q(f)df \quad (32)$$

where Δf is the noise bandwidth in Hertz, $E(f)$ is the input voltage, $q(f)$ is the relative response of the selective filter and f_1 and f_2 are nominally the half-power points.

III.2. DETERMINATION OF NOISE BANDWIDTH*

Figure 17 is a typical filter curve. The noise bandwidth of such a filter is given by

$$\Delta f = \frac{1}{P} \int_{f_1}^{f_2} E^2(f)q(f)df \quad (33)$$

and can be determined by our equipment. If the TP-627 analyzer is connected to the TP-633 power integrator, and a sine wave is applied to the input, the output of the power integrator will be $E^2(f)q(f)$ (fig. 18). By carefully varying the frequency of the sine wave, we can obtain a maximum indication; this will be $E_{\max}^2 = P$. The output signal can be normalized to $P = 50\%$ by adjusting the system gain. The TP-626 oscillator will sweep the frequency intervals shown in table IV in 100 sec. The time constant of the integrator in the TP-633 is set at 100 sec; therefore the instrument integrates the squared signal between f'_1 and f'_2 in 100 sec, f'_1 and f'_2 are frequencies at the integration limits, chosen well outside the passband of the filter from the data in table IV. As an example, consider a filter of 200-Hz bandwidth between the half-power points. We would choose a 480-Hz integration interval and would set the 200-Hz passband in the center of this range. A sine wave of 1000 Hz is applied to the TP-627, and a SLOW scan rate on the $\times 10$ range is chosen. Then

$$f'_1 = 1000 - \frac{480}{2} = 760 \text{ Hz}$$

$$f'_2 = 1000 + \frac{480}{2} = 1240 \text{ Hz}$$

The TP-626 is set to scan from 760 to 1240 Hz with the aid of an EPUT meter. Suppose the TP-633 meter reading to be 20%. Then the noise bandwidth would be 40% of 480-Hz, which is

*This method of noise bandwidth determination is most convenient for our particular analyzer system. Other methods employing graphical integration are described in references 31 and 33.

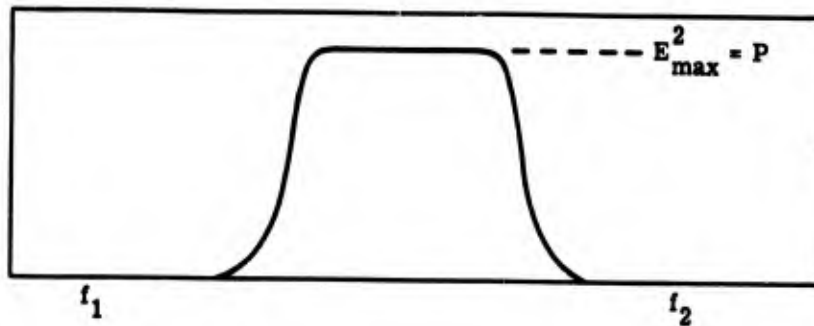


FIGURE 17. TYPICAL FILTER CURVE

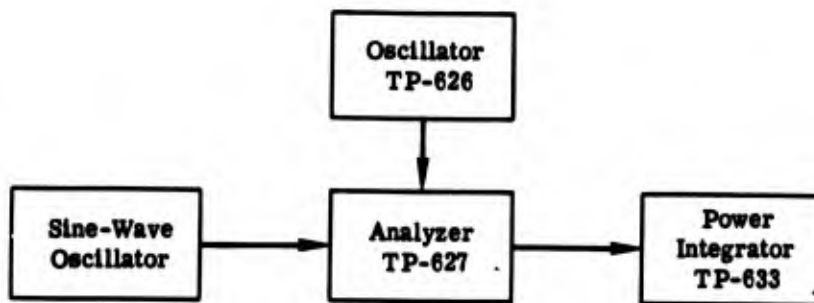


FIGURE 18. CALIBRATION BLOCK DIAGRAM

TABLE IV. TP-626 OSCILLATOR SWEEP INTERVALS PER 100 SECONDS

SLOW SPEED

- 4.8 Hz on $\times 1$ range (0-250 Hz)
- 48 Hz on $\times 10$ range (0-2500 Hz)
- 480 Hz on $\times 100$ range (0-25,000 Hz)

FAST SPEED

- 48 Hz on $\times 1$ range (0-250 Hz)
- 480 Hz on $\times 10$ range (0-2500 Hz)
- 4800 Hz on $\times 100$ range (0-25,000 Hz)

WILLOW RUN LABORATORIES

192.0 Hz. The meter reading is multiplied by 2 since the system has been normalized to a maximum value of 50%. The noise bandwidth values for the filters in the spectrum analyzer on hand were calculated in this way (table III). The frequency response of each filter is presented as figures 19-21 for comparison. The data given in table V were used to adjust the bandwidth divisors for automatic division of the mean square signal by the noise bandwidth of the filter.

TABLE V. BANDWIDTH DIVISOR SETTINGS

Filter Number	Nominal Bandwidth (Hz)	Effective Square Bandwidth (Hz)	Square Root of Bandwidth (Hz ^{1/2})	Attenuator Setting	Bandwidth Attenuator Setting
1	2	2.88	1.70	27.0 × 1/100	45.9 × 1/100
2	20	24.5	4.96	27.0 × 1/100	13.4 × 1/10
3	200	206.4	14.35	27.0 × 1/100	38.75 × 1/10

III.3. SAMPLE MEASUREMENTS

After the noise bandwidths of the filters were calculated in this manner and the bandwidth divisors adjusted accordingly, the following check was made to insure proper operation. A signal from a noise generator,* which was essentially flat in the region 20-25,000 Hz, was applied to the wave analyzer. The amplitude of the signal y(t) was set at 0.7 v rms or 0.5 v² (mean square). The PSD for the input signal was then

$$P_f(f) = \frac{0.5 v^2}{24,980} \cong 2 \times 10^{-5} [v^2 - Hz^{-1}] \quad (34)$$

Substituting equation 26 for the standard error into equation 27 and rearranging,

$$P_f < (f, \Delta f, T) > = \frac{P_f(f)}{1 \pm \sqrt{T_d \Delta f}} \quad (35)$$

For the 2-Hz filter (with an RC constant, K = 10 sec) we would expect

$$P_f < (f, \Delta f, T) > = \frac{2 \times 10^{-5}}{1 \pm \frac{1}{\sqrt{T} \Delta f}} = \frac{2 \times 10^{-5}}{1 \pm \frac{1}{\sqrt{20}}} = \frac{2 \times 10^{-5}}{1 \pm 0.22}$$

or

$$1.64 \times 10^{-5} \leq P_f < (f, \Delta f, T) > \leq 2.56 \times 10^{-5} [v^2 - Hz^{-1}] \text{ (68\% confidence)}$$

*General Radio Model 1390-B.

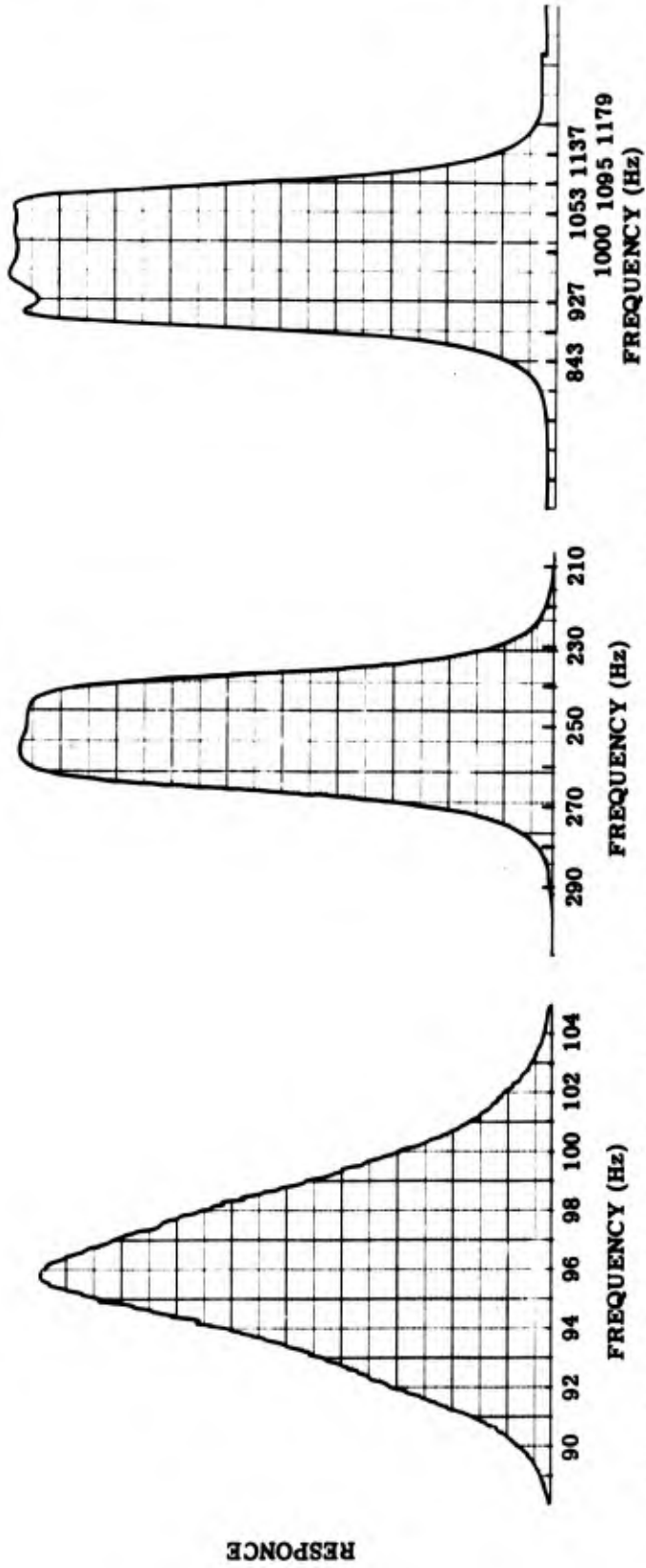


FIGURE 19. RESPONSE OF 2-Hz FILTER FIGURE 20. RESPONSE OF 20-Hz FILTER FIGURE 21. RESPONSE OF 200-Hz FILTER

WILLOW RUN LABORATORIES

The observed values (fig. 22) are

$$P_f < (f, \Delta f, T) >_{\text{obs}} = \frac{0.5 \text{ v}^2 \text{-Hz}^{-1}}{(\text{gain})^2} \times (\% \text{ deflection on L \& N Recorder})$$

$$= \frac{0.5}{10^4} (0.45 \pm .07) \text{ (about 68\% of time)}$$

or

$$1.90 \times 10^{-5} \leq P_f < (f, \Delta f, T) >_{\text{obs}} \leq 2.60 \times 10^{-5} \text{ v}^2 \text{-Hz}^{-1}$$

which is fairly close to anticipated values.

For the 20-Hz filter (K = 4 sec) we would expect

$$P_f < (f, \Delta f, T) >_{\text{calc}} = \frac{2 \times 10^{-5}}{1 \pm \frac{1}{\sqrt{80}}} = \frac{2 \times 10^{-5}}{1 \pm 0.112}$$

or

$$1.88 \times 10^{-5} \leq P_f < (f, \Delta f, T) >_{\text{calc}} \leq 2.25 \times 10^{-5} \text{ v}^2 \text{-Hz}^{-1}$$

and

$$P_f < (f, \Delta f, T) >_{\text{obs}} = \frac{0.5}{10^4} (0.39 \pm 0.03)$$

or

$$1.80 \times 10^{-5} \leq P_f < (f, \Delta f, T) >_{\text{obs}} \leq 2.10 \times 10^{-5} \text{ v}^2 \text{-Hz}^{-1}$$

Finally, for the 200-Hz filter (K = 4 sec) we would expect .

$$P_f < (f, \Delta f, T) >_{\text{calc}} = \frac{2 \times 10^{-5}}{1 \pm \frac{1}{\sqrt{800}}} = \frac{2 \times 10^{-5}}{1 \pm 0.035}$$

or

$$1.93 \times 10^{-5} \leq P_f < (f, \Delta f, T) >_{\text{calc}} \leq 2.07 \times 10^{-5} \text{ v}^2 \text{-Hz}^{-1}$$

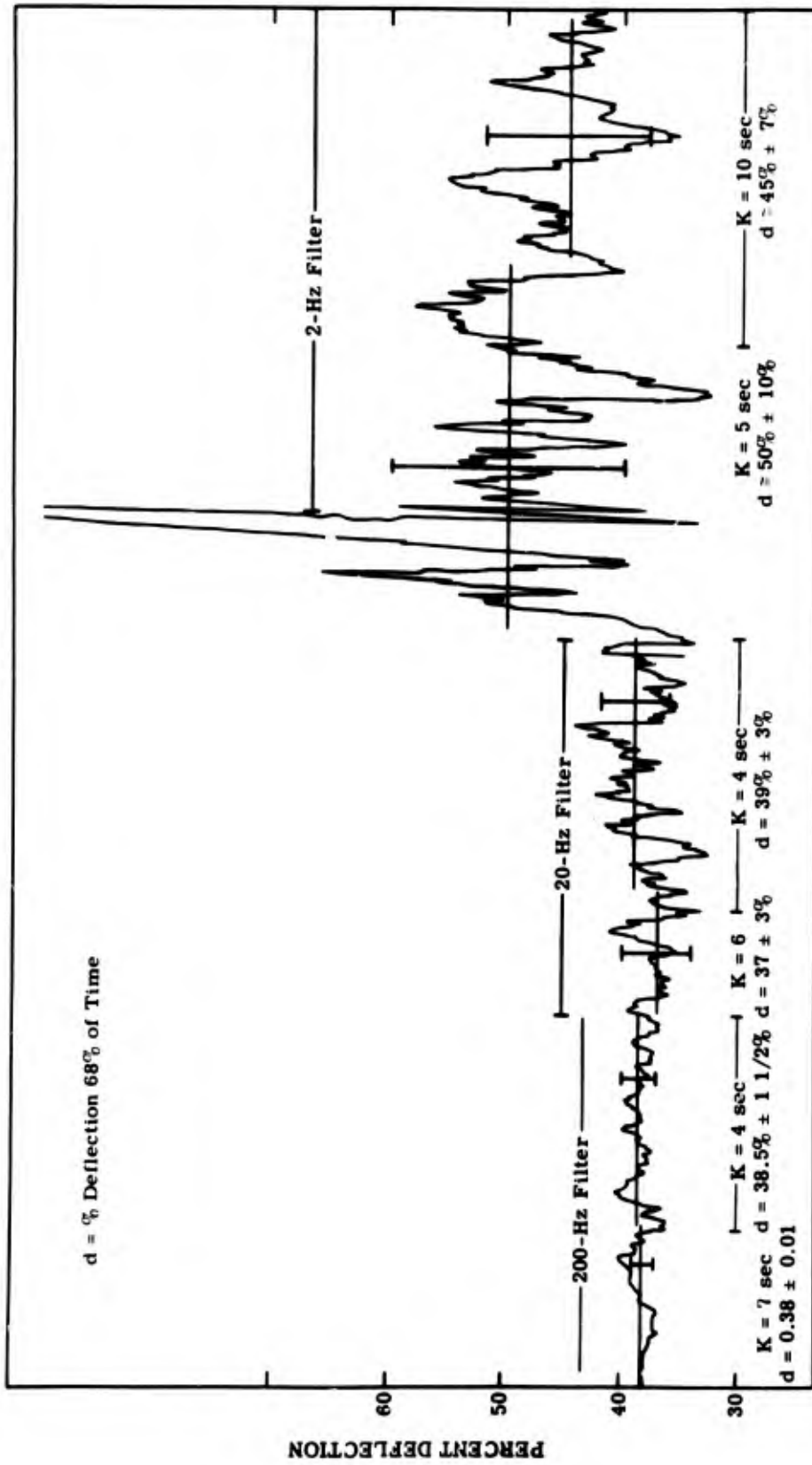


FIGURE 22. POWER SPECTRAL DENSITY MEASUREMENTS FOR THREE FILTERS

WILLOW RUN LABORATORIES

and

$$P_f \langle (f, \Delta f, T) \rangle_{\text{obs}} = \frac{0.5}{10^4} (0.385 \pm 0.015)$$

or

$$1.85 \times 10^{-5} \leq P_f \langle (f, \Delta f, T) \rangle_{\text{obs}} \leq 2 \times 10^{-5} \text{ v}^2 \text{-Hz}^{-1}$$

Note that, as the filter becomes narrower, it is necessary to increase the integration time to obtain a suitable reading. For most PSD measurements, the bandwidth divisor circuit is probably adequately calibrated, but for more stringent requirements, a readjustment of the circuit is advisable. This entails an entire reevaluation of the effective square bandwidths and therefore was not performed.

WILLOW RUN LABORATORIES

REFERENCES

1. J. B. Edson, Optical Studies of the Jet Flame of the V-2 Missile in Flight, BRL Report No. 708, Ballistic Research Laboratories, Aberdeen Proving Ground, Md., 1949.
2. A. B. C. Anderson, A Jet-Tone Orifice Number for Orifices of Small Thickness-Diameter Ratio, NOTS 854 NAVORD Report 2096, Naval Ordnance Test Station, China Lake, Calif.
3. A. B. C. Anderson, Structure and Velocity of the Periodic Vortex-Ring Flow Pattern of a Primary Pfeifenton (Pipe Line) Jet, NOTS 1436 NAVORD Report 5237, Naval Ordnance Test Station, China Lake, Calif., April 1955; also J. Acoust. Soc. Am., Vol. 27, No. 6, November 1955, pp. 1048-1053.
4. A. B. C. Anderson, "Vortex-Ring Structure Transition in a Jet Emitting Discrete Acoustic Frequencies," J. Acoust. Soc. Am., Vol. 28, No. 5, September 1956, pp. 914-921.
5. M. R. Krasno and J. L. Ruby, "A-C Radiometry in the 8 to 14 Micron Region," Proc. IRIS, Vol. IX, No. 3, September 1964, pp. 71-75.
6. F. C. Harshbarger and M. Dorian, Some Studies of the Fluctuations in Emission From the Exhaust Gases of Small Rocket Motors, Report No. ZPH-130, Convair Div., General Dynamics Corp., San Diego, Calif., 1961.
7. D. J. Baker, J. R. M. Arendt, and T. P. Condron, Optical Radiation from Missile Plumes and Shockwaves, Monthly Progress Report No. 32, Electrodynamics Laboratories, Utah State University, Logan, Utah, 15 May 1963.
8. M. Harwit, Measurement of Fluctuations in Radiation from a Source in Thermal Equilibrium, MIT, Naval Supersonic Lab., and RLE, Tech. Report 364 (DSc Thesis) June 1960 (AD 246-390).
9. J. J. Adler, A Measurement of Propeller-Modulated Radiation from Eight Different Small Aircraft, Report No. IDP-954, U. S. Naval Ordnance Test Station, China Lake, Calif., 21 July 1960.
10. D. A. Merrell, "Modulated Electric Flare," Proc. IRIS, Vol. VII, No. 2, August 1962, pp. 91-94.
11. B. N. Edwards and R. R. Steen, "Effects of Atmospheric Turbulence on the Transmission of Visible and Near Infrared Radiation," Appl. Opt., Vol. 4, No. 3, March 1965.
12. R. Paulson, E. Ellis, and N. Ginsburg, I: Research Concerning Infrared Emissivity; II: Atmospheric Optical Noise Measurements, Report No. AFCRL-62-869, Syracuse University, Dept. of Physics, Syracuse, N. Y., August 15, 1962.
13. C. W. Jones, Design and Construction of a Rocket-Borne Radiometer for Measurement of Plume Modulation, Report No. SR3, Block Associates, Inc., Cambridge, Mass., October 1960.
14. R. C. Jones, The Study of IR Backgrounds by the Wiener Spectrum Method, unpublished report, Infrared Laboratory, Institute of Science and Technology, The University of Michigan, Ann Arbor, 1960.
15. J. S. Bendat, Principles and Applications of Random Noise Theory, Wiley, 1958.
16. R. B. Blackman and J. T. Tukey, The Measurements of Power Spectra, Dover, 1958.

WILLOW RUN LABORATORIES

17. W. B. Davenport and W. L. Root, Random Signals and Noise, McGraw-Hill, 1958.
18. L. R. Burrow, Jr., Some Analog Methods for Power Spectral Density Analysis, Reprint No. 1.5-3-65, Instrument Society of America, Los Angeles, Calif., October 4-7, 1965.
19. R. C. Moody, Considerations in the Analysis of Random Wave Processes, Memorandum, Technical Products Co., Los Angeles, Calif.
20. A. G. Piersol, The Measurement and Interpretation of Ordinary Power Spectra for Vibration Problems, Report No. NAS A CR-90, National Aeronautics and Space Administration, Washington, D. C., September 1964.
21. R. C. Jones, "Performance of Detectors for Visible and Infrared Radiation," Adv. Electron., Vol. V, pp. 1-96, Academic, 1953.
22. M. R. Holter et al., Fundamentals of Infrared Technology, Macmillan, 1962.
23. F. E. Nicodemus and G. J. Zissis, Methods of Radiometric Calibration, Report No. 4613-201-R, Institute of Science and Technology, The University of Michigan, Ann Arbor, October 1962.
24. W. Wallin, "Wave Synthesizing Light Chopper," J. Opt. Soc. Am., Vol. 45, No. 4, 1955, p. 287.
25. Hewlett Packard Associates Technical Data Sheets 4104, 4105.
26. S. B. Gibson et al., Characteristics of Gallium Arsenide Diodes As Infrared Radiation Sources, U. S. Army Research and Development Laboratories, Fort Belvoir, Va., September 1965, AD 624 129.
27. D. Burch, D. Gryvnak, and D. Williams, Infrared Absorption by Carbon Dioxide, RF Project 778, Scientific Report II, The Ohio State University, Research Foundation, Columbus, Ohio, January 1961.
28. P. Schumacher, The Emissivity of the Rocketdyne Circular Aperture Blackbody Radiation Source, Research Report No. 63-3, Rocketdyne Div. of North American Aviation Inc., Canoga Park, Calif., February 1963.
29. C. T. Morrow, "Averaging Time and Data-Reduction Time for Random Vibration Spectra: I" J. Acoust. Soc. Am., Vol. 30, No. 5, 1958, p. 456.
30. C. T. Morrow, "Averaging Time and Data-Reduction Time for Random Vibrations Spectra: II," J. Acoust. Soc. Am., Vol. 30, No. 6, 1958, p. 572.
31. J. S. Bendat, L. D. Enochson, and A. G. Piersol, Analytical Study of Vibration Data Reduction Methods, Technical Products Co., Los Angeles, Calif., September 1963.
32. C. T. Morrow and R. B. Muchmore, "Shortcomings of Present Methods of Measuring and Simulating Vibration Environments," J. Appl. Mech., Vol. 77, 1965, p. 367.
33. Operation Manual for TP-625 Wave Analyzer System, Technical Products Co., Los Angeles, Calif.

UNCLASSIFIED

Security Classification

DOCUMENT CONTROL DATA - R&D

(Security classification of title, body of abstract and indexing annotation must be entered when the overall report is classified)

1 ORIGINATING ACTIVITY (Corporate author) Willow Run Laboratories, Institute of Science and Technology, The University of Michigan, Ann Arbor		2a REPORT SECURITY CLASSIFICATION Unclassified	
		2b GROUP	
3 REPORT TITLE MEASUREMENT OF THE TIME-VARYING COMPONENT OF RADIATION FROM INFRARED SOURCES			
4 DESCRIPTIVE NOTES (Type of report and inclusive dates)			
5 AUTHOR(S) (Last name, first name, initial) Hall, E. C., Fecteau, M. L., and Roe, C. L.			
6 REPORT DATE May 1968		7a TOTAL NO OF PAGES vi + 48	7b NO OF REFS 33
8a CONTRACT OR GRANT NO. SD-91		9a ORIGINATOR'S REPORT NUMBER(S) 4613-105-T	
b. PROJECT NO.		9b OTHER REPORT NO(S) (Any other numbers that may be assigned this report)	
c.			
d.			
10 AVAILABILITY/LIMITATION NOTICES This document has been approved for public release and sale; its distribution is unlimited.			
11. SUPPLEMENTARY NOTES		12. SPONSORING MILITARY ACTIVITY Advanced Research Projects Agency, Department of Defense, Washington, D. C.	
13 ABSTRACT Techniques for the calibration of a temporal radiometer have been studied. The calibration described for either periodic or random fluctuations utilizes sinusoidally modulated radiation from a blackbody. A complete description is given of the data acquisition and analysis facilities which were assembled for this study and used to calibrate a test radiometer. The practical aspects of spectral analysis (including the interplay among filter bandwidth, scan rate, data sample length, and averaging time) are discussed, and a technique for measuring the noise equivalent bandwidth of the frequency-selective filter in the spectrum analyzer is described.			

DD FORM 1473
1 JAN 64

UNCLASSIFIED
Security Classification

14. KEY WORDS	LINK A		LINK B		LINK C	
	ROLE	WT	ROLE	WT	ROLE	WT
Infrared radiation Temporal radiometry Calibration						

INSTRUCTIONS

1. **ORIGINATING ACTIVITY:** Enter the name and address of the contractor, subcontractor, grantee, Department of Defense activity or other organization (*corporate author*) issuing the report.
- 2a. **REPORT SECURITY CLASSIFICATION:** Enter the overall security classification of the report. Indicate whether "Restricted Data" is included. Marking is to be in accordance with appropriate security regulations.
- 2b. **GROUP:** Automatic downgrading is specified in DoD Directive 5200.10 and Armed Forces Industrial Manual. Enter the group number. Also, when applicable, show that optional markings have been used for Group 3 and Group 4 as authorized.
3. **REPORT TITLE:** Enter the complete report title in all capital letters. Titles in all cases should be unclassified. If a meaningful title cannot be selected without classification, show title classification in all capitals in parenthesis immediately following the title.
4. **DESCRIPTIVE NOTES:** If appropriate, enter the type of report, e.g., interim, progress, summary, annual, or final. Give the inclusive dates when a specific reporting period is covered.
5. **AUTHOR(S):** Enter the name(s) of author(s) as shown on or in the report. Enter last name, first name, middle initial. If military, show rank and branch of service. The name of the principal author is an absolute minimum requirement.
6. **REPORT DATE:** Enter the date of the report as day, month, year, or month, year. If more than one date appears on the report, use date of publication.
- 7a. **TOTAL NUMBER OF PAGES:** The total page count should follow normal pagination procedures, i.e., enter the number of pages containing information.
- 7b. **NUMBER OF REFERENCES:** Enter the total number of references cited in the report.
- 8a. **CONTRACT OR GRANT NUMBER:** If appropriate, enter the applicable number of the contract or grant under which the report was written.
- 8b, 8c, & 8d. **PROJECT NUMBER:** Enter the appropriate military department identification, such as project number, subproject number, system numbers, task number, etc.
- 9a. **ORIGINATOR'S REPORT NUMBER(S):** Enter the official report number by which the document will be identified and controlled by the originating activity. This number must be unique to this report.
- 9b. **OTHER REPORT NUMBER(S):** If the report has been assigned any other report numbers (*either by the originator or by the sponsor*), also enter this number(s).
10. **AVAILABILITY/LIMITATION NOTICES:** Enter any limitations on further dissemination of the report, other than those

imposed by security classification, using standard statements such as:

- (1) "Qualified requesters may obtain copies of this report from DDC."
- (2) "Foreign announcement and dissemination of this report by DDC is not authorized."
- (3) "U. S. Government agencies may obtain copies of this report directly from DDC. Other qualified DDC users shall request through _____."
- (4) "U. S. military agencies may obtain copies of this report directly from DDC. Other qualified users shall request through _____."
- (5) "All distribution of this report is controlled. Qualified DDC users shall request through _____."

If the report has been furnished to the Office of Technical Services, Department of Commerce, for sale to the public, indicate this fact and enter the price, if known.

11. **SUPPLEMENTARY NOTES:** Use for additional explanatory notes.
12. **SPONSORING MILITARY ACTIVITY:** Enter the name of the departmental project office or laboratory sponsoring (*paying for*) the research and development. Include address.
13. **ABSTRACT:** Enter an abstract giving a brief and factual summary of the document indicative of the report, even though it may also appear elsewhere in the body of the technical report. If additional space is required, a continuation sheet shall be attached.

It is highly desirable that the abstract of classified reports be unclassified. Each paragraph of the abstract shall end with an indication of the military security classification of the information in the paragraph, represented as (TS) (S) (C) or (U)

There is no limitation on the length of the abstract. However, the suggested length is from 150 to 225 words.

14. **KEY WORDS:** Key words are technically meaningful terms or short phrases that characterize a report and may be used as index entries for cataloging the report. Key words must be selected so that no security classification is required. Identifiers, such as equipment model designation, trade name, military project code name, geographic location, may be used as key words but will be followed by an indication of technical context. The assignment of links, rules, and weights is optional.